國 立 交 通 大 學

電機學院微電子奈米科技產業研發碩士班

碩 士 論 文

低臨限電壓與高驅動電流之薄膜電晶體在金屬鋁與介電層氧

化鑭鉿上之研究

Low Threshold Voltage and High Drive Current Poly-Silicon Thin Film

Transistors Using Aluminum Metal Gate and HfLaO Dielectric

研 究 生：黃群懿

指導教授：荊鳳德　教授

中 華 民 國 九 十 七 年 一 月

低臨限電壓與高驅動電流之薄膜電晶體在金屬鋁與介電層氧化鑭鉿上之研究

Low Threshold Voltage and High Drive Current Poly-Silicon Thin Film Transistors Using Aluminum Metal Gate and HfLaO Dielectric

研 究 生：黃群懿　　　　　Student：Chen-Yi Huang

指導教授：荊鳳德　　　　　Advisor：Dr. Albert Chin

國 立 交 通 大 學

電機學院微電子奈米科技產業研發碩士班

碩 士 論 文

A Thesis

Submitted to College of Electrical and Computer Engineering

National Chiao Tung University

in partial Fulfillment of the Requirements

for the Degree of

Master

in

Industrial Technology R & D Master Program on

Microelectronics and Nano Sciences

January 2008

Hsinchu, Taiwan, Republic of China

中華民國九十七年一月

低臨限電壓與高驅動電流之薄膜電晶體在金屬鋁與介電層氧化鑭鉿上之研究

研究生: 黃群懿　　　　　　　　　　　　指導教授: 荊鳳德 教授

國立交通大學電機學院產業研發碩士班

摘要

本論文將高介電常數的氧化鑭鉿整合至低溫多晶矽薄膜電晶體當作閘極氧化層，並且選用鋁來作為金屬閘極在 LTPS 上。將可得到高驅動電流、低臨界電壓和低次臨界斜率，大大提升了元件的特性。不僅如此，也因此而達成高的開/關電流比例及閘極崩潰電場。上述所得之優秀的特性與所使用的閘極氧化層種類有密切關係。

使用氧化鑭鉿作為閘極氧化層，可造成高閘極電容密度與很小的等效氧化層厚度。有別於一般的 TFT 元件，此種元件並不需使用一些介面鈍化處理或是特別的結晶步驟，只需要用爐管就可以達到成晶的目的了。

Low Threshold Voltage and High Drive Current

Poly-Silicon Thin Film Transistors Using Aluminum Metal

Gate and HfLaO Dielectric

Student: Chen-Yi Huang   **Advisor: Dr. Albert Chin**

Industrial Technology R & D Master Program of
Electrical and Computer Engineering College
National Chiao Tung University

Abstract

We have integrated a Metal gate into Low temperature Poly-Silicon(LTPS) thin-film transistors (TFTs) with high- κ gate dielectric. We used Aluminum for metal gate, and we used HfLaO for high-κ gate dielectric on LTPS. We got high drive current, low threshold voltage and low sub-threshold slop to improve the performance of device obviously. It also achieved high on/off ratio and high gate breakdown electric field. The excellent performances mentioned above are related closely to gate dielectric.

We used HfLaO for high-κ dielectric and it can product high density gate capacitor and less EOT. This kind of device is different from other common devices because it is not necessary to apply passive treatment or specific process of crystallization. We only used furnace to crystallize.

誌　謝

Contents

Chapter 3: The experimental steps and Device Characterization

Chapter 4: Result & Discussion

Chapter 5: Conclusion

Chapter 1
Introduction

1.1 Overview of Polycrystalline Silicon Thin-Film Transistors Technology

The thin film transistors (TFTs) are widely used in a flat-panel display, in which light must be able to pass through the substrate material to reach the viewer. A Silicon wafer is opaque and obviously will not allow light to transmit through it. Glass is the most commonly used starting substrate because it is highly transparent and is compatible with conventional semiconductor processing steps. Since glass is not a semiconductor like silicon, a thin film of silicon is deposited on top and the transistors are fabricated using this thin layer. Hence, we call "thin-film transistor."

The thin film transistor technology is similar to the conventional metal oxide semiconductor field effect transistor (MOSFET). Both of them are contain layers of semiconductor, dielectric, and conductive thin films, and are fabricated with semiconductor process. However, there are still some differences between these two devices. In the MOSFETs, the channel region is formed in the single crystal silicon wafer. Several high-temperature process steps, such as oxide growth, dopant annealing, and epitaxy growth, are involved in the the fabrication of MOSFETs. The bulk film and film-film interface

properties are stabilized and determined by the highest process temperature. In contrast to

MOSFETs, all thin film layers of TFTs are deposited including the active region. With the

glass whose melting temperature is lower than $600^{\circ}C$, all thin film deposition process need to

be executed in low temperature.

The most significant advantages of amorphous silicon TFTs are their low-cost and

low temperature process technologies. The low-temperature process allows circuits to be

fabricated on low-cost and large size glass substrates. However, the low current-driving

capability of a-Si TFTs limits their applications to low-gain and low-speed circuits. Therefore,

the interest in polycrystalline silicon thin film transistor technology has increased extensively

in recent years.

Traditionally, AMLCDs were fabricated using hydrogentated amorphous silicon

(a-Si:H)TFTs for the pixel switching devices. The a-Si:H TFTs have many advantages,

particularly its compatibility with low temperature process on large glass substrate and high

off-state resistivity which result a low leakage current. However, the low electron field effect

mobility in a-Si:H TFTs has limited the technology development for AMLCDs application.

To integrate the switching elements with the driving circuits on the same substrate is very

desirable not only to reduce the cost but also to improve the system performance. Therefore,

poly-Si TFTs, which provide higher electron field effect mobility, have been developed as a

lower photocurrent, CMOS capability and better reliability, thus enables the integration of peripheral circuits as well as the active-matrix switching elements on the same substrate.

It should be noted that "poly-Si" covers a range of thin film materials, which vary in the methods of preparation, grain size and nature, distribution of intragranular and bulk defects, and surface roughness. Thus, the properties of any particular film will be dependent on these parameters, which have therefore been the subject of extensive studies to optimize key TFTs parameters such as off-current, on-current, subthreshold swing and mobility. The performance of poly-Si TFTs is strongly influenced by grain boundaries and intragranular defects. In order to enhance TFTs electrical characteristics, several techniques which are used to increase the grain sizes of poly-Si films have been proposed. The methods for recrystallization of a-Si to poly-Si at glass-compatible temperatures are the key technology for fabricating low-temperature process (LTP) poly-Si TFTs on glass. It was reported that the a-Si film can be recrystallized by several techniques, such as: solid-phase crystallization (SPC), excimer laser annealing (ELA), metal-induce lateral crystallization (MILC), and rapid thermal annealing (RTA) to obtain larger grain sizes of poly-Si for high mobility.

1.2 Overview of high-κ gate dielectrics

Many materials systems are currently under consideration as potential replacements

for SiO₂ as the gate dielectric material for sub-0.1 mm complementary metal–oxide–semiconductor (CMOS) technology. A systematic consideration of the required properties of gate dielectrics indicates that the key guidelines for selecting an alternative gate dielectric are (a) permittivity (b) band-gap (c) band alignment to silicon (d) thermodynamic stability (e) film morphology (f) interface quality (g) compatibility with the current or expected materials to be used in processing for CMOS devices (h) process compatibility (i) reliability [1]-[6]. Many dielectrics appear favorable in some of these areas, but very few materials are promising with respect to all of these guidelines. Specifically, a dielectric constant $(\kappa)\sim 25$ is required to satisfy the requirements for CMOS gate dielectrics leading out to years beyond 2010. Similar or larger values are required for dielectrics used in embedded dynamic random access memory (DRAM) cells and radiofrequency (RF) coupling capacitors. The material must also respond positively to a series of other demands relating to such effects as lack of interactivity with the Si substrate, low leakage currents, low interface state density, high electrical barriers against charge injection, etc. The gate leakage current through the gate oxide increases significantly because direct tunneling is the primary conduction mechanism in down-scaling CMOS technologies. Therefore, the engineering of high-κ gate dielectrics have attracted great attention and played an important role in VLSI technology.

In the case of increasing the gate capacitance, consider a parallel plate capacitor (ignoring quantum mechanical and depletion effects from a Si substrate and gate):

$$C = \frac{k \in_0 A}{t}$$

(1)

Where κ is the dielectric constant (also referred to as the relative permittivity in this article) of the material, $\in_0$ is the permittivity of free space (= 8.85×10^{-3} fF/μm), A is the area of the capacitor, and t is the thickness of the dielectric. This expression for C can be rewritten in terms of t_{eq} (i.e., equivalent oxide thickness) and κ_{ox} (=3.9, dielectric constant of SiO$_2$) of the capacitor. The term t_{eq} represents the theoretical thickness of SiO$_2$ that would be required to achieve the same capacitance density as the dielectric (ignoring issues such as leakage current and reliability). For example, if the capacitor dielectric is SiO$_2$, $t_{eq} = 3.9\in_0$ (A/C), and a capacitance density of C/A = 34.5 fF/μm2 corresponds to t_{eq} = 10 Å. Thus, the physical thickness of an alternative dielectric employed to achieve the equivalent capacitance density of t_{eq} = 10 Å can be obtained from the expression

$$\frac{t_{eq}}{k_{ox}} = \frac{t_{high-k}}{k_{high-k}}$$

(2a)

or simply,

$$t_{high-k} = \frac{k_{high-k}}{k_{ox}} t_{eq} = \frac{k_{high-k}}{3.9} t_{eq}$$

(2b)

A dielectric with a relative permittivity of 16 therefore affords a physical thickness of ~40 Å to obtain t_{eq} = 10 Å. (As noted above, actual performance of a CMOS gate stack does not scale directly with the dielectric due to possible quantum mechanical and depletion effects.)

According to the ITRS (International Technology Roadmap for Semiconductor)[7], the suitable gate dielectrics must have κ value more than 8 for 50-70 nm technology nodes and that must be more than 15 when the technology dimension less than 50 nm.

Research on finding an appropriate substitute to the superior SiO_2 has been going on for almost a decade. Oxy-nitrides (SiOxNy) have been introduced to extend the use of SiO_2 in production but eventually it has to be replaced by a high-κ material, such as Ta_2O_5, TiO_2, HfO_2, ZrO_2, Al_2O_3, La_2O_3 or mixtures of them or metal-oxide-silicates of the mentioned compounds. However, most metal oxides will have the characteristics of crystallization at elevated temperature which cause devices generate non-uniform leakage distribution and give large statistical variation for nano-meter devices across the chip. Therefore, replacement gate strategies have been proposed to prevent crystallization and deleterious effects of mass and electrical transport along grain boundaries.

1.3 Motivation

The dimension of poly-Si TFTs needs to be scaled down to increase the aperture ratio in TFTs array and also the driving speed in peripheral circuits. However, small dimensional effects including short channel effects and narrow width effect influence device characteristics seriously. Good control of device performance isessential for the realization of applying these small dimension poly-Si TFTs. Compared to MOSFETs and SOIs, only a few studies had focused on the small dimension poly-Si TFTs. Whereas the behaviors of short channel poly-Si TFTs are even more complicated than MOSFETs and SOIs due to the poly-Si channel film. Moreover, due to the presence of abundant grain boundary trap states, n-channel poly-Si TFTs are found to exhibit more severe impact ionization effects and the floating body effects than its silicon-on-insulator (SOI) counterparts.

To prevent from short channel effect in high speed transistors, thickness of gate oxide continues shrinking. With this condition, we first encounter the difficulty of uniformity of thin film. Next, on characteristic of device, we will encounter: (1) direct tunneling, which make large leakage current. (2) mobility degradation, surface scattering raises on account of increasing vertical electric field with thickness shirking. To solve the problem above, scientists use high dielectric constant material that get thicker physical thickness with the same EOT as silicon oxide for gate dielectric film.

In this thesis, we use Sputtering (PVD)-HfLaO for gate dielectric film. The HfLaO combines the the high dielectric constant of HfO_2 (~25) and the ability of La_2O_3 of tunning the work function of metal over it. The performance is due to the increase, by a factor of $\kappa_{dielectric}/\kappa_{SiO_2}$, in the gate capacitance density. This lowers the threshold voltage and improves both the gate-leakage current and breakdown field, since the thickness of the high dielectric constant layer can be increased. And PVD (Physical Vapor Deposition) process is not higher than 600°C, which is very suitable for TFTs process.

1.4 Thesis Outline

This thesis is organized into the following chapters:

In chapter 1, firstly, a brief overview of poly-Si TFTs technology and its various applications are introduced. Then, we will describe the high-κ material in the development of CMOS, paving the way for applying it in the field of thin film transistor. Finally, we give the motivation for the necessity of high-κ insulated thin film transistors.

In chapter 2, some basis about semiconductor and thin film transistor are briefly introduced. Besides, some critical process related to thin film transisitor are also included in this chapter.

In chapter 3, the preparation of devices in our work is described, including the step of poly-Si TFTs fabrication process, measuring tools we used to evaluate our performance and methods to extract device parameters such as threshold voltage, subthreshold swing, field effect mobility, and ON/OFF current ratio.

In chapter 4, results of this experiment are shown including ON/OFF ratio, typical transfer (I_D-V_G) and output (I_D-V_D) characteristics for different Lanthanide content in the high-κ insulator.

At last, the conclusions of our work are given in the chapter 5.

Chapter 2
Basic Device Physics

2.1 Energy band in silicon

In a silicon crystal each atom has four valence electrons to share with its four nearest neighboring atom. The valence electrons are shared in a paired configuration called a covalent bond. The most important result of the application of quantum mechanics to the description of electrons in a solid is that the allowed energy levels of electrons will be grouped into bands (Kittel, 1976). The bands are separated by regions of energy that the electrons in the solid cannot possess: forbidden gaps. The highest energy band that is completely filled by electrons at 0 ^{o}K is called the valence band. The next higher energy band, separated by a forbidden gap from the valence band, is called the *conduction band*, as shown in Fig 2.1. , the energy of the electrons in the conduction band increases upward, while the energy of the holes in the valence band increases downward. The bottom of the conduction band is designated E_c, and the top of the valence band E_v. Their separation, or the bandgap, is $E_g = E_c - E_v$. For silicon, E_g is 1.12eV at room temperature or 300 ^{o}K. The bandgap decreases slightly as the temperature increases, with a temperature increases, with a temperature coefficient of $dEg / dT \doteqdot$ - 2.73 $\times$ 10^{-4} eV/^{o}K for silicon near 300 ^{o}K (Arora, 1993).

2.2 n-type and p-type silcon

Intrinsic silicon at room temperature has an extremely low free-carrier concentration; therefore, its resistivity is very high. In practice, intrinsic silicon hardly exists

at room temperature, since it would require materials with an unobtainably high purity. Most impurities in silicon introduce additional energy levels in the forbidden gap and can be easily ionized to add either electrons to the conduction band or holes to the valence, depending on where the impurity level is (Kittel, 1976). The electrical conductivity of silicon is then dominated by the type and concentration of the impurity atoms, or dopants, and the silicon is called extrinsic.

Silicon is a column-IV element with four valence electrons per atom. There are two types of impurities in silicon that are electrically active: those from column-V such as arsenic or phosphorus, and those from column-III such as boron. As is shown in Fig 2.2, a column-V atom in a silicon lattice tends to have one extra electron loosely bonded after forming covalent bonds with other silicon atoms. In most cases, the thermal energy at room temperature is sufficient to ionize the impurities are called donors; they become positively charged when ionized. Silicon material doped with column-V impurities or donors is called n-type silicon, and its electrical conductivity is dominated by electrons in the conduction band. On the other hand, a column-III impurity atom in a silicon lattice tends to be deficient by one electron when forming covalent bonds with other silicon atoms (Fig 2.2). Such an impurity atom can also be ionized by accepting an electron from the valence band, which leaves a free-moving hole that contributes to electrical conduction. These impurities are called acceptors; they become negatively charged when ionized. Silicon material doped with column-III impurities or acceptors is called p-type silicon, and its electrical conductivity is dominated by holes in the valence band. It should be noted that impurity atoms must be in a substitutional site (as opposed to interstitial) in silicon in order to be electrically active.

In terms of the energy-band diagrams in Fig 2.3 (a) and Fig 2.3 (b), donors add allowed electron states in the band-gap close to the conduction-band edge, while acceptors add allowed states just above the valence-band edge. Donor levels contain positive charge

when ionized (emptied). Acceptor levels contain negative charge when ionized (filled). The ionization energies are denoted by $E_c - E_d$ for donors and $E_a - E_v$ for acceptors, respectively. Phosphorus and arsenic are commonly used donors, or n-type dopants, with low ionization energies on the order of 2kT, while boron is a commonly used acceptor or p-type dopant with a comparable ionization energy. Arsenic, boron, and phosphorus have the highest solid solubility among all the impurities, which makes them the most important doping species in VLSI technology.

2.3 Energy-band diagram of an MOS system

The metal-oxide-semiconductor (MOS) structure is the basis of CMOS technology. The Si-SiO2 MOS system has been studied extensively(Nicollian and Brews, 1982) because it is directly related to most planar devices and integrated circuits.

The cross section of an MOS capacitor is shown in Fig 2.4. It consists of a conducting gate electrode (metal or heavily doped polysilicon) on top of a thin layer of silicon dioxide grown on a silicon substrate. The energy-band diagrams of the three components are shown in Fig 2.5 Silicon dioxide is an insulator with a large energy gap in the range of 8-9eV.

It is convenient to relate the band structures of all three materials to a common reference potential, the vacuum level. The vacuum level is defined as the energy level at which the electron is free, i.e., no longer bonded to the lattice. In silicon, the vacuum level is 4.05eV above the conduction band. In other words, an electron at the conduction-band edge

must gain a kinetic energy of 4.05eV (called the electron affinity, χ) in order to break loose from the crystal field of silicon. In silicon dioxide, the vacuum level is 0.95eV above its conduction band, which means that the potential barrier is 4.05eV－0.95eV = 3.1eV between the conduction bands of silicon and silicon dioxide. This figure has important significance when discussing the reliability of Si-SiO$_2$ systems.

In metals, the energy difference between the vacuum level and the Fermi level is called the work function of the metal. Different metals have different work functions.

2.4.1 Flat band and accumulation

When there is no applied voltage between the metal and silicon, their Fermi levels line up. Since the work functions are equal, their vacuum levels line up as well, and the bands in both the silicon and oxide are flat, as shown in Fig 2.6(a). This is called the flat-band condition. There is no charge, no field, and the carrier concentration is at the equilibrium value throughout the silicon. Now consider the case when a negative voltage is applied to the gate of a p-type MOS capacitor, as shown in Fig 2.6(b). This raises the metal Fermi level with respect to the silicon surface in the same direction as the oxide field. Because of the low carrier concentration in silicon (compared with metal), the bands bend upward toward the

oxide interface. The Fermi level stays flat within the silicon, since there is no net flow of

conduction current. The potential at the silicon surface is called the surface potential. Due to

the band bending, the Fermi level at the surface is much closer to the valence band than is the

Fermi level in the bulk silicon. This is referred to as the accumulation condition. One can

think of the equal amount of negative charge appears on the metal side of the MOS capacitor,

as required for charge neutrality.

2.4.2 Depletion and Inversion
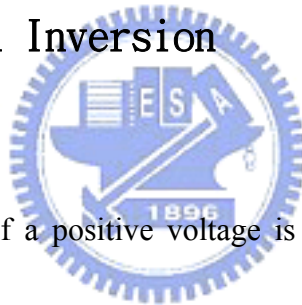
On the other hand, if a positive voltage is applied to the gate of a p-type MOS

capacitor, the metal Fermi level moves downward which creates an oxide field in the direction

of accelerating a negative charge toward the metal electrode. A similar field is induced in the

silicon, which causes the bands to bend downward toward the surface, as shown in Fig 2.6(c).

Since the valence band in the bulk, the hole concentration at the surface is lower than the

concentration in the bulk. This is referred to as the depletion condition. One can think of the

holes as being repelled away from the surface by the positive gate voltage. The depletion of

holes at the surface leaves the region with a net negative charge arising from the unbalanced

acceptor ions. An equal amount of positive charge appears on the metal side of the capacitor.

As the positive gate voltage increases, the band bending also increases, resulting in a wider depletion region and more (negative) depletion charge. This goes on until the bands bend downward so much that the intrinsic potential (near the mid-gap) at the surface becomes lower than the Fermi potential, as shown in Fig 2.6(d). When this happens, all the holes are depleted from the surface, and the surface potential is such that it is energetically favorable for electrons to populate the conduction band. Note that this n-type surface is formed not by doping, but instead by inverting the original p-type substrate with an applied electric field. This condition is called inversion. The negative charge in the silicon consists of both the ionized acceptors and the thermally generated electrons in the conduction band. Again, it is balanced by an equal amount of positive charge on the metal gate. The surface is inverted as soon as $E_i = (E_c+E_v) / 2$ crosses E_f. This is called weak inversion because the electron concentration remains small until E_i is considerably below E_f. If the gate voltage is increased further, the concentration of electrons at the surface will be equal to, and then exceed, the hole concentration in the substrate. This condition is called strong inversion.

2.5 MOSFET Devices

The metal-oxide-semiconductor field effect transistor is the building block of VLSI circuit in microprocessors and dynamic memories. The basic structure of a MOSFETs is shown in Fig 2.7. It is a four terminal devices with the terminals designated as gate, source,

drain, and body. A n-channel MOSFETs consists of a p-type silicon substrate into which two n$^+$ regions, the source and the drain are formed. The gate electrode is usually made of metal or heavy doped polysilicon and is separated from the substrate by a thin silicon oxide. The surface region under the gate oxide between the source and drain is called channel region and is critical for current conduction in MOSFETs. The basic operation of a MOSFETs device can be easily understood from the MOS capacitor discussed in the previous section. When there is no voltage applied to the gate, there is no current flow between the source and drain. When a sufficiently large positive voltage in applied to the gate, the silicon surface is inverted to n-type, which form a conduction channel between the n$^+$ source and drain. If there is a voltage between them, an electron current will flow from the source to the drain.

2.6 Thin Film Transitor Devices
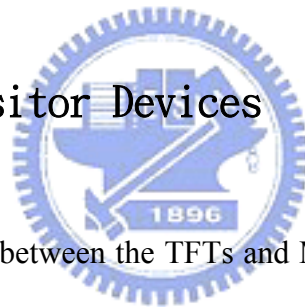
The main difference between the TFTs and MOSFETs is the channel material. The former is made of amorphous silicon or polycrystalline silicon while the latter is made of single crystalline material. The a-Si or poly-Si exist many crystallites that has any type of orientation that means a break in the crystal form one crystallite to the other. The atoms at the border of a crystallite are also linked to the neighbor crystallite ones. However, these atoms bonds are disoriented rather than a prefect lattice of silicon. This border is called a grain boundary. The break in the lattice at grain boundary creates a break in the periodicity of the potential in the material, and create new energy states in the band gap of silicon, which can govern the electrical behavior of the film and consequently of the devices based on the polycrystalline material. The grain boundaries act as energy barriers that the carriers have to overcome. The smaller the grain are, the more grain boundary the film contains and the lower the conductivity becomes. For better performance, the a-Si of the active region need to be

transform to poly-Si. We call this process "poly-Si recrystallization.

2.7 Poly-Silicon Recrystallization

In order to increase TFTs performance, various techniques have been used for crystallize a-Si. Historically, solid phase crystallization was the first technology to produce poly-Si films for display applications, followed by rapid thermal annealing crystallization process, metal-induce lateral crystallization process, and laser annealing crystallization. These four major methods of recrystallization are describe as follow:

2.7.1 Solid-Phase Crystallization Process Technology

The most direct method of obtaining poly-Si films from initially amorphous precursor-Si films is via SPC (Solid-Phase Crystallization) in a furnace environment. Amorphous silicon is a thermodynamically metastable phase possessing a driving force for transformation to polycrystalline phase given sufficient energy to overcome the initial energy barrier. Solid-phase crystallization can be accomplished within a wide annealing temperature range that requires a similarly wide range of annealing times. The relationship between annealing upon the microstructural details of the precursor-Si film, different annealing times have been observed at the same annealing temperature. A key factor affecting crystallization is the nucleation rate in the precursor-Si film. The nucleation rate is strongly influenced by the selected deposition method and conditions. The structural order/disorder in the precursor film

affects the ability of the film to form supercritical nuclei when subjected to thermal annealing. The structural order is, in turn, affected by deposition parameters such as temperature and deposition rate. As the temperature decreases and the deposition rate decreases, films are formed having a higher degree of structural disorder.

Despite the successes of traditional SPC methods in increasing grain size and reducing crystallization temperature, the crystallization time typically required for complete transformation tends to be rather long. The crystallization-time issue is further compounded by the use of PECVD as the deposition method for the precursor-Si film. The selection of this technique, even though suboptimal, has been driven by the prior application of PECVD technology in a-Si TFT fabrication.

2.7.2 Metal-Induce Lateral Crystallization Process Technology

Recently, the metal-induced lateral crystallization (MILC) process has been studied widely for polycrystalline silicon thin film transistor applications. Compared with the conventional solid-phase crystallization process of amorphous silicon, MILC process offers the advantages of lower annealing temperature and better crystallization film. In addition, poly-Si films crystallized by the MILC process can be used as the basis for developing the low cost integrated circuits on glass substrate. At present, nickel and palladium have been used to induce lateral crystallization of a-Si:H film. Experimental annealing temperatures and MILC rates obtained for Ni and Pd, respectively. However, the annealing temperature

(<=500°C) is still too high for poly-Si TFT devices to be fabricated on conventional glass substrate, and the low MILC rate, gold (Au) has been employed to induce lateral crystallization of a-Si:H film owing its lower eutectic temperature (363°C). The crystallization of Au/a-Si:H film is observed starting from annealing treatment at 175°C, which is a much lower crystallized temperature than for Ni and Pd (500°C). After the discovery of Au-MILC where microtwin-free Si grains are obtained, MILC also has been successfully applied to the low-temperature fabrication of high-mobility N-channel TFTs.

2.7.3 Rapid Thermal Annealing Crystallization Process Technology

To obtain the poly-Si crystalline phase, laser crystallization can be used with very good results, but the process is expensive and difficult to control. On the other hand, for similar results, furnace annealing requires lower temperature and is much simple, can be better checked, and is cheaper. So, to achieve desirable material properties for the poly-Si films, RTA has been used in this work, thermal crystallization of amorphous silicon. For the Si films annealed at 750°C or higher, using RTA, the grain average sizes are reduced whereas the electron/hole mobility are increased. This indicates that the poly-Si film electrical properties depend not only on the grain size, but also on the crystalline quality of the grains.

Moreover, it appears that the large amount of crystalline defects remaining in the so-called "grains" of the films annealed at 600°C (SPC) are partially annihilated when the films are annealed at higher temperatures. With regards to the TFTs electrical characteristics, the work suggests combining SPC and RTA steps to obtain TFTs with improved electrical performance.

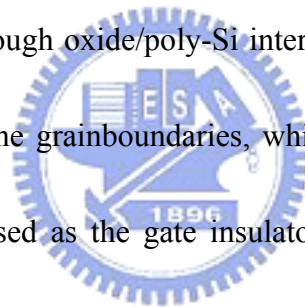## 2.7.4 Excimer Laser Annealing Crystallization Process Technology

Pulsed excimer laser annealing is also being investigated as an alternative crystallization technique to replace furnace annealing. For fabricating high performance poly-Si TFTs on a glass substrate, excimer laser crystallization method is very promising for the following reasons. First, it is a low-temperature process introduced no serious thermal shrinkage of the glass substrate caused by the effects of the short pulse and large absorption coefficient of silicon in the UV light regime. Secondly, it can crystallize the film selectively by partially irradiating the film surface, so both poly-Si TFTs and amorphous Silicon TFTs can be formed on the same substrate. The laser process heats the thin silicon film to the melting point on a short time scale (tens of nanoseconds) that allows the film to melt and recrystallized without significantly heating the glass substrate. Since this process achieves higher annealing temperatures than a conventional furnace annealing, significantly

higher-quality poly-Si films can be obtained.

2.8 Dielectric Material for Poly-Silicon Applications

Dielectric materials control many essential functions in the fabrication, the operation, and the reliability of gate insulated field effect transistors (FETs), such as MOSFETs and especially for a TFT that fabricated on a glass substrate. Dielectrics of various properties are prepared for different applications, such as diffusion barrier, thermal barrier, and electrical insulator. A good insulator material should satisfy at least two requirement. The first requirement is its electrical insulation property. Ideally, the conductance has to be null. In reality, electrical charges can flow through the insulator under various conditions, which correspond to the leakage current in the device. The other requirement is good dielectric performance under operation condition. The TFT's threshold voltage, subthreshold slope and field effect mobility depend directly on charges present in the bulk of the gate insulator and at the gate insulator-semiconductor interface. The most popular dielectrics for semiconductor devices are silicon dioxide and silicon nitride. Other materials, such as high-κ metal based or rare earth based oxide, have been used for a thicker layer. Recently, several methods for deposition of gate dielectric were investigated such as plasma-enhanced chemical vapor deposition (PECVD), electron cyclotron resonance (ECR) plasma thermal oxide, liquid phase

deposited (LPD) oxide. PECVD system which has good step coverage, high deposition rate,

low temperature process at 300^oC.The PECVD widely used for the deposition of many kinds

of films such as silicon dioxide (using TEOS+O_2 as the source gases), silicon nitride,

oxide/nitride/oxide (ONO) stack films (in-situ deposition). The tetraethylorthosilicate (TEOS)

can be decomposed below 300^oC by the enhancement effects of plasma or ozone. TEOS

silicon dioxide films were demonstrated superior step coverage at low temperature. However,

the deposited TEOS oxide has a higher leakage current, lower breakdown voltage, and higher

instability than thermal oxide due to the low integrity and high interface trapped charges. The

deposited oxide also has the rough oxide/poly-Si interface due to the localized enhancement

of oxidant diffusion through the grainboundaries, which leads to higher local electric field.

HfLaO, a prospect material used as the gate insulator in the study of MOSFET has good

property such as high dielectric constant, high thermal stability, and low defect density. For

the first time, we use it in the TFTs and acquire good device characteristics, making it a

promising material to realize system on panel (SOP).
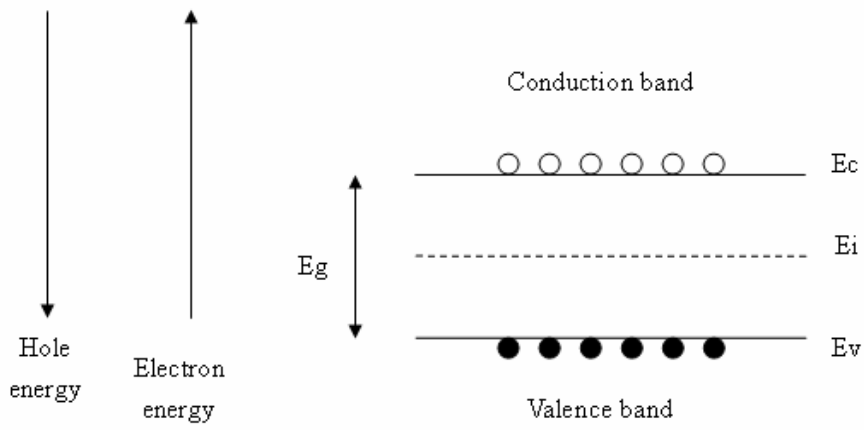
Fig 2.1

Fig 2.2

Fig 2.3(a)

Fig 2.3(b)

Silicon dioxide

Gate electrode

tox

Silicon substrate

Fig 2.4

0.95 eV

Ec

$q\chi = 4.05$ eV

$q\Phi m = 4.1$eV

$q\Phi_s$

$q\Phi_s$

Ef

Ec

Metal(aluminum)

Eg=1.12eV

$q\Psi_B$

8~9 eV

Ei

Ef

Ev

Silicon (p-type)

Ev

Silicon dioxide

Fig 2.5

Flat-band

Vg = 0

Vg = 0

Ec

Ef

Ef

Ec

Ef

Ef

Ev

Ev

P-type

N-type

Fig 2.6(a)

Accumulation

Vg < 0

Vg > 0

Ef

Ec

Ec

Ef

Ef

Ef

Ev

Ef

Ev

P-type

N-type
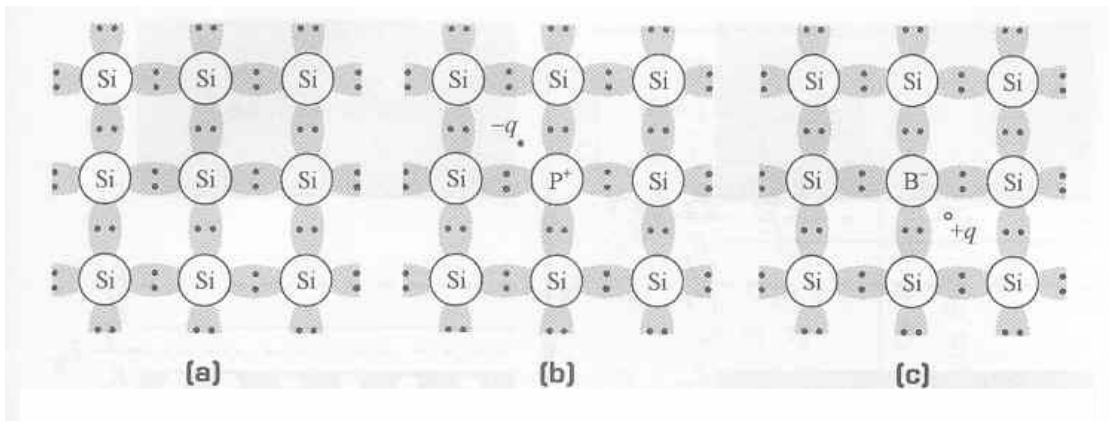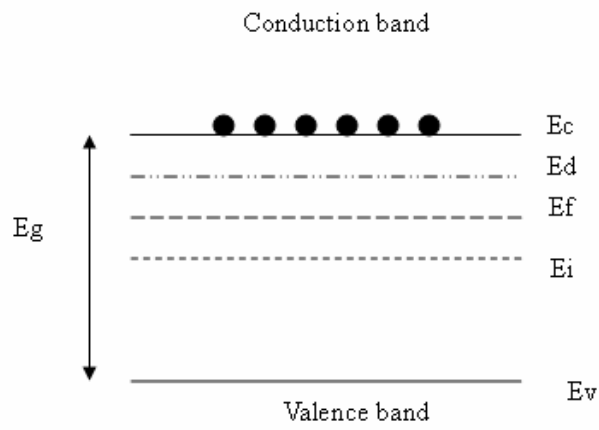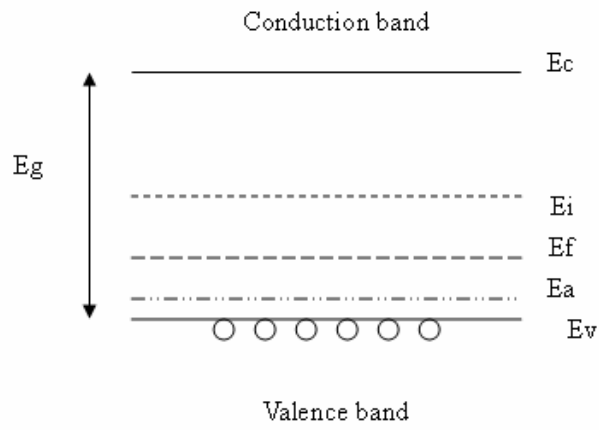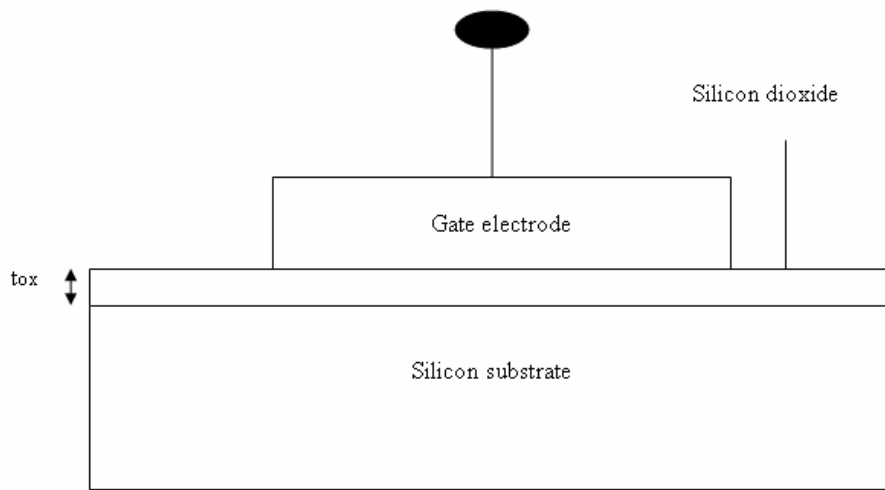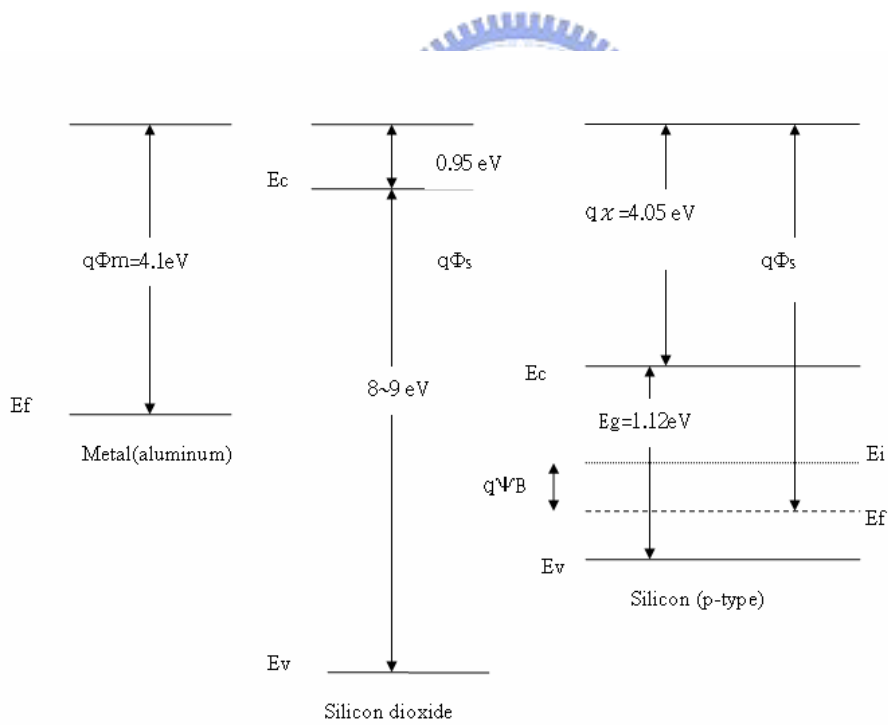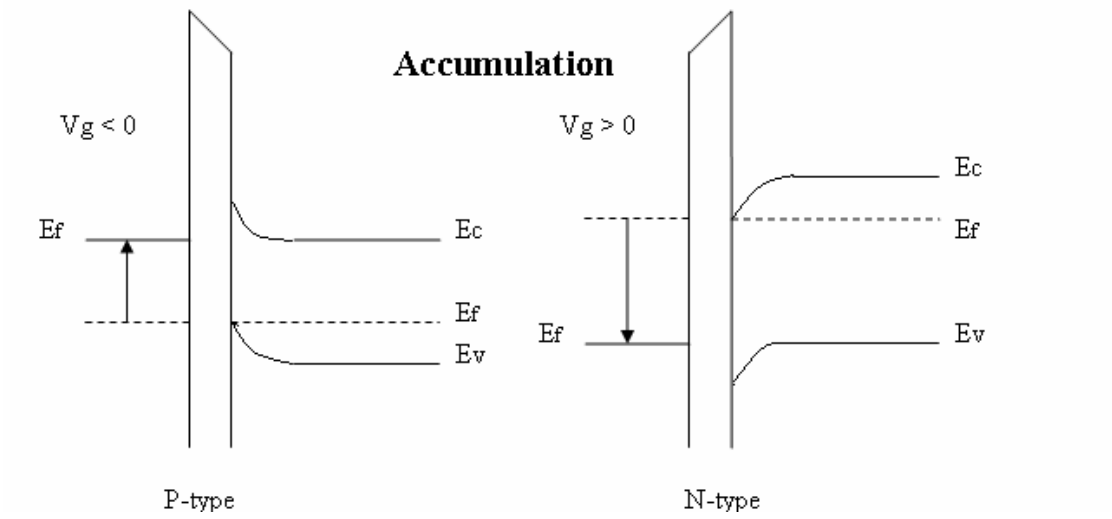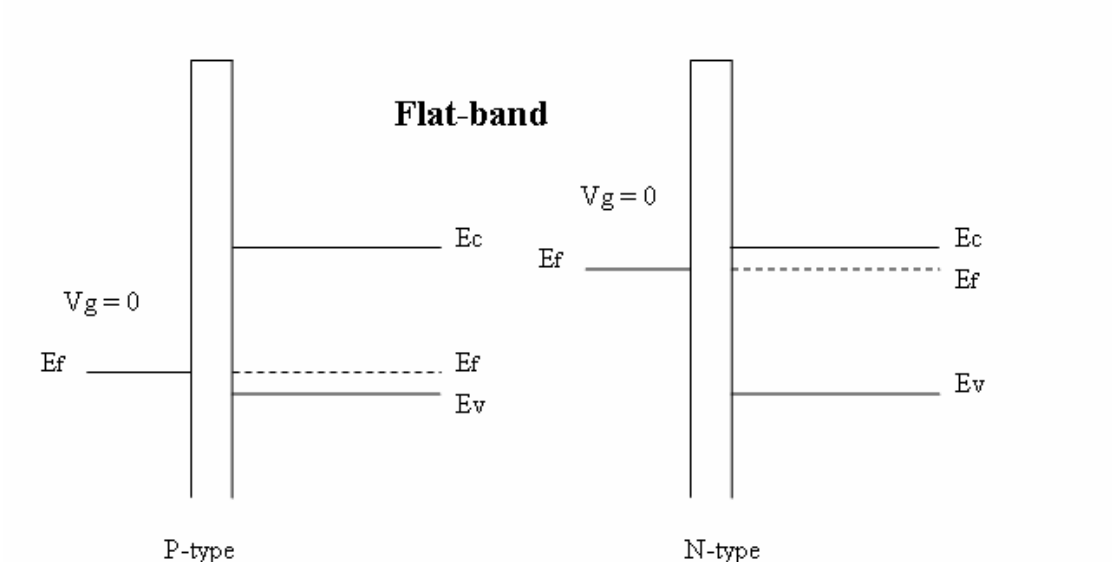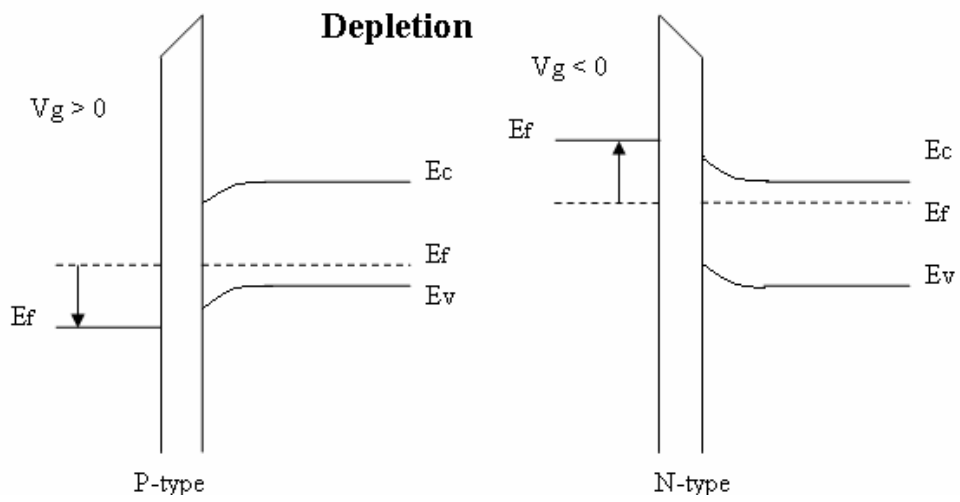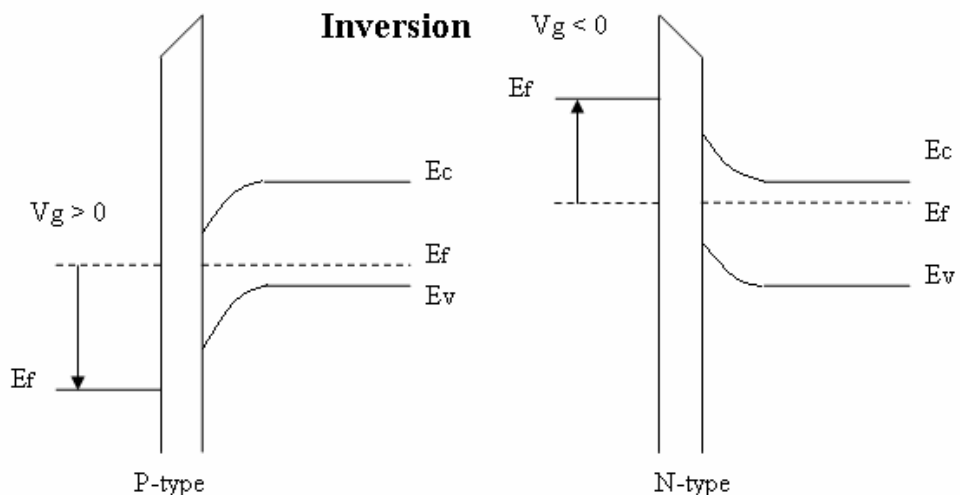
Fig 2.6(b)

Fig 2.6(c)

Fig 2.6(d)
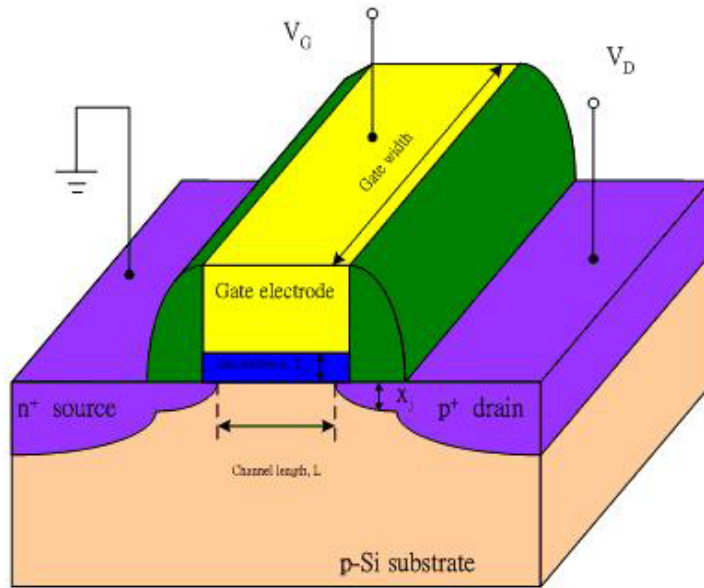
Fig 2.7

Chapter 3
The Experimental Steps and Device Characterization

3.1 Device Fabrication Process

In this study we use a silicon wafer with 500nm wet oxide on it, which is to demonstrate the glass substrate. Fabrication of the TFTs started with the formation of a Poly-Silicon film, by depositing 100nm amorphous Silicon on SiO_2/Si wafers (using LPCVD at 550^oC). After a $600\ ^oC$ and 20 hours annealing in N_2 ambient, amorphous silicon was recrystallization to become poly-Si. For device isolation, 500nm oxide was deposited by PECVD and device active region was defined by photolithography and wet etching in BOE for about 5 min. The source and drain regions in the active device region were formed by ion-implantation   with phosphorus (35KeV at 5×10^{15} cm^{-2}) and activated at $600\ ^oC$ for 12 hours annealing in N_2 ambient. The second mask was used to remove the PECVD oxide in the gate region, and again RCA clean was done to assure the high-κ/poly-Si interface. 50nm thick HfLaO was deposited by PVD as the gate dielectric, following by a $500\ ^oC$ Post deposition annealing (PDA). Then gate was formed by depositing 150nm Al using PVD. Finally, the TFTs devices were completed by gate definition with lift-off process after electrode formation. The completed devices were under $400\ ^oC$ sintering for 30 min in N_2 ambient to enhance the device performance. The fabricated device has gate length and width of 10 μm and 100 μm, respectively.

3.2 Measurement Tools

In this study, devices were put on the stage of probe station (Fig 3.14) to be measured. Capacitance-voltage(C–V) and current-voltage(I–V) characteristics were obtained using HP4284 (Fig 3.15) and HP4156 (Fig 3.16), respectively. The current – voltage characteristic measurement of thin film transistor devices was performed by HP4156 semiconductor parameter analyzer with source grounded and body floating. The thickness of dielectric is measured by Ellipometer.

3.3 Parameter Extraction

In this section, the methodology we use to extract typical parameters in TFTs such as threshold voltage, subthreshold swing, field-effect mobility μFE, and the on/off current ratio for device characteristics are briefly introduced.

3.3.1 Determination of Threshold Voltage

Threshold voltage (V_{th}) is an important parameter because it affect the drain current and device drivability drastically. There are several methods to determine the threshold voltage of thin film transistors. Two of most commonly used extraction methods are the

constant drain current method and the maximum transconductance method. The constant

drain current method define the voltage at a specific drain current   as the threshold voltage.

Typically, the threshold current is specified at (W/L) ×10nA for V_{DS}=0.1V and (W/L) ×

100nA for V_{DS} =5V   in most papers to extract the threshold voltage of TFTs. , where W and

L are channel width and channel length, respectively. However, in this thesis we use

maximum transconductance method to get our threshold voltage because it is more accurate.

This techniques is the linear extrapolation method with the drain current measured as a

function of gate voltage at a low drain voltage of 50~100mV to ensure operation in the linear

region, and the drain current as a function   of   gate voltage   can   be   reduced   to

$$I_{DS} = \mu_{eff} C_{ox} \left(\frac{W}{L}\right)\left[\left(V_{GS} - V_{th}\right)V_{DS}\right]$$----------------(Eq. 4.1)

The drain current is not zero when V_{GS} below threshold voltage and approaches zero

asymptotically. Hence the I_{DS} versus V_{GS} curve can be extrapolated to I_D=0, and the V_{th} is

determined from the extrapolated intercept of gate voltage Equation (4.1) is strictly only valid

for negligible series resistance. Fortunately series resistance is usually negligible at the low

drain current when threshold voltage measurements are made. The I_{DS}-V_{GS} curve deviates

from a straight line at gate voltage below V_{th} due to sub-threshold current and above V_{th} due

to series resistance and mobility degradation effects. It is common practice to find the point of

maximum slope of the I_{DS}-V_{GS} curve and fit a straight line to extrapolate to I_D=0 by means of

finding the point of maximum of transconductance (G_m).

3.3.2 **Determination of Field Effect Mobility**

The field-effect mobility (μ_{FE}) is determined from the transconductance g_m at low drain voltage. Usually, the maximum value of transconductance (G_m) are used to represent the device performance. The transfer characteristics of Poly-Silicon TFTs are similar to those of conventional MOSFETs, so that the first order of I-V relation in the bulk Si MOSFETs can be applied to Poly-Silicon TFTs. The drain current in linear region ($V_{DS} < V_{GS} - V_{th}$) can be approximated as the following equation:

$$I_{DS} = \mu_{eff} C_{ox} \left(\frac{W}{L}\right) \left[\left(V_{GS} - V_{th}\right) V_{DS} - \frac{1}{2} V_{DS}^2 \right] \text{-----------------(Eq. 4.2)}$$

where Cox is the gate oxide capacitance per unit area, Vth is the threshold voltage, and W and L are channel width and channel length, respectively. Therefore, the transconductance is given by

$$g_m = \frac{\partial I_{DS}}{\partial V_{GS}} = \mu_{eff} C_{ox} \left(\frac{W}{L}\right) V_{DS} \text{---------------------------(Eq. 4.3)}$$

Therefore, the field-effect mobility is

$$\mu_{eff} = \frac{L}{C_{ox} W V_{DS}} g_{m(max)} \Big|_{V_{DS} \to 0} \text{--------------------(Eq. 4.4)}$$

3.3.3 Determination of Sub-threshold Slope

Sub-threshold slope (S.S.) is a typical parameter to describe the control ability of gate toward channel, which reflects the turn on/off speed of a device. It is defined as the amount of gate voltage required to increase/decrease drain current by one order of magnitude. The S.S. should be independent of drain voltage and gate voltage. However, in reality, the S.S. increases with drain voltage due to channel shortening effect such as charge sharing, avalanche multiplication and punchthrough effect. The sub-threshold slope is also related to gate voltage due to undesirable and inevitable factors such as the serial resistance and interface states. In this thesis, the S.S. is defined as one-third of the gate voltage required to decrease the threshold current by three orders of magnitude. The threshold current is specified to be the drain current when the gate voltage is equal to threshold voltage.

3.3.4 Determination of ON/OFF Current Ratio

On/Off current ratio is one of the most important parameters of poly-Si TFTs especially in the application of LCD because It affects the bright and dark states of TFTs screens drastically. The leakage current mechanism in poly-Si. TFTs is like that in MOSFETs.

But, in MOSFETs, the channel is composed of single crystalline Si and the leakage current is due to the tunneling of minority carrier from drain region to accumulation layer located in channel region. In poly-Si TFTs, the channel is composed of poly-Si. A large amount of trap state densities in grain structure attribute a lot of defect states in energy band gap to enhance the tunneling effect. Therefore, the leakage current is much larger in poly-Si TFTs than in MOSFETs. When the voltage drops between gate voltage and drain voltage increases, the band gap width decreases and the tunneling effect becomes much more severe. Normally we can find this effect in typical Poly-Silicon TFT's I_{DS}-V_{GS} characteristics where the magnitude of leakage current will reach a minimum and then increase as the gate voltage decreases/increases for n/p-channel TFTs. There are a lot of ways to specify the on and off-current. In this chapter, take n-channel poly-Si TFTs for examples, the on-current is defined as the drain current when gate voltage at the maximum value and drain voltage is 0.1V. The off-current is specified as the minimum current when drain voltage equals to 0.1V.
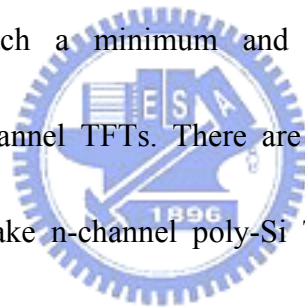
$$\frac{I_{on}}{I_{off}} = \frac{Maximum\ Current\ of\ I_{DS} - V_{GS}\ Plot\ at\ V_{DS} = 0.1V}{Minimum\ Current\ of\ I_{DS} - V_{GS}\ Plot\ at\ V_{DS} = 0.1V}\ \text{-------------}\textbf{(Eq.4.5)}$$

1. Silicon substrate (RCA Clean)
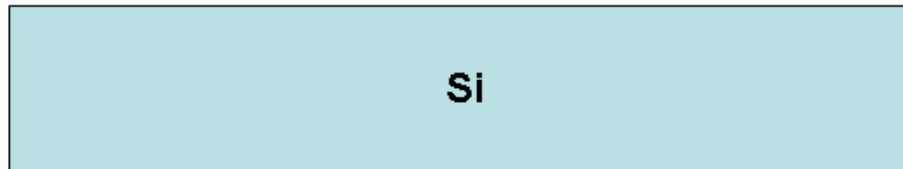
Fig 3.1 Step1

2. Wet oxide growth (500nm)

Fig 3.2 Step2

3. Amorphous Silicon deposition by LPCVD at 550 ^{o}C
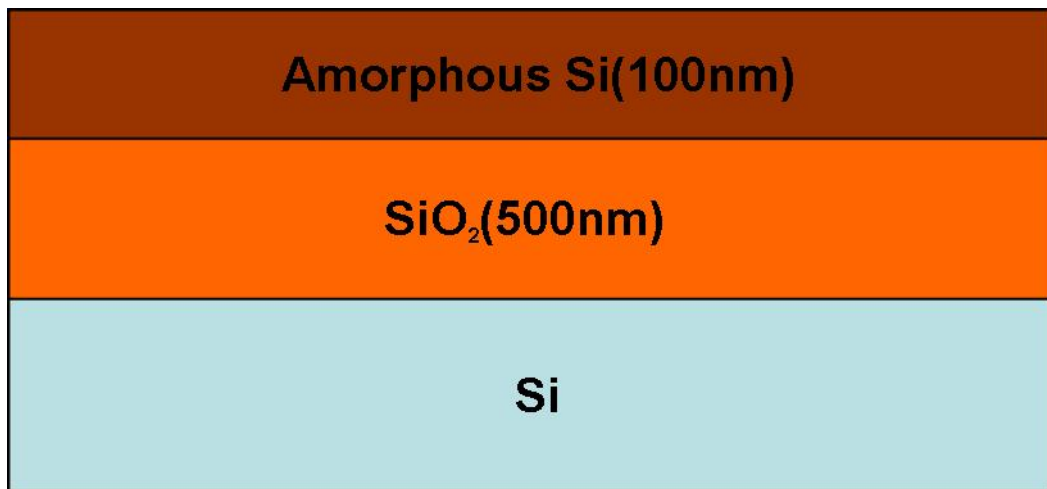
Fig 3.3 Step3

4. Poly-Silicon recrystallization by annealing in N$_2$ at 600 ^{o}C for 20hr in furnace

Fig 3.4 Step4
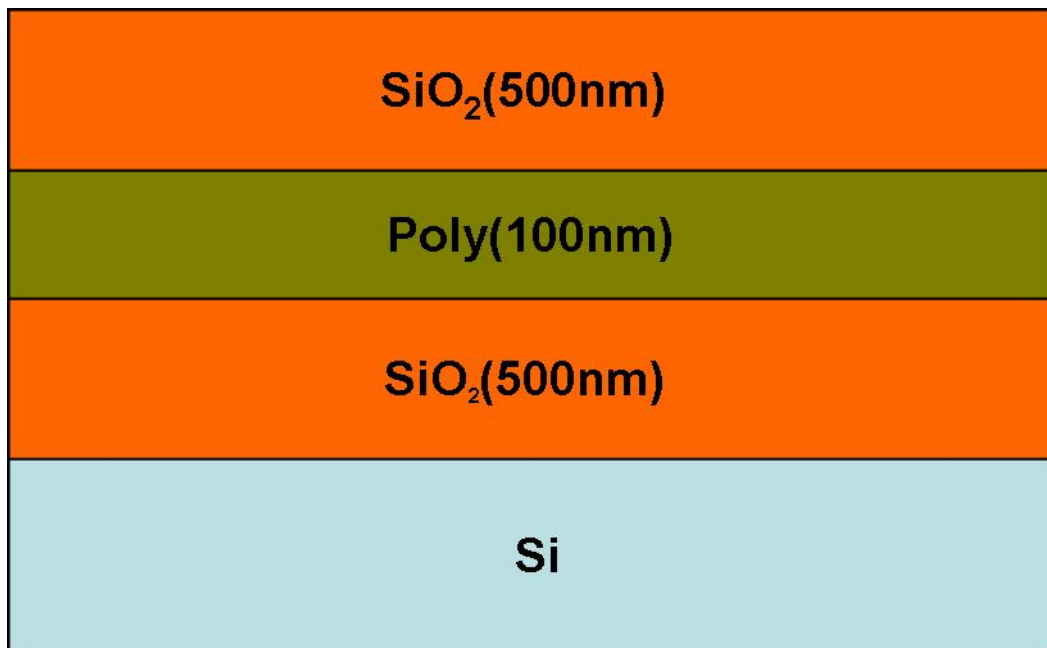
5. Isolation oxide deposition by PECVD (500nm)

Fig 3.5 Step5

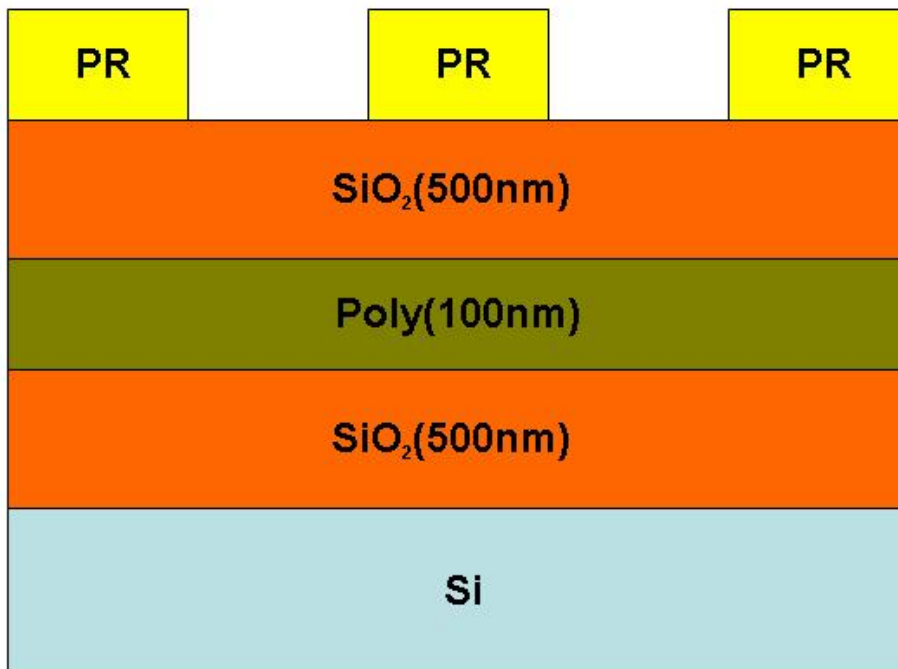**6. Source and Drain region define, patterning, etching(MASK-1)**

Fig 3.6 Step6

7. Source and Drain implantation with phosphorus(35kev at 5E15 cm^{-2})
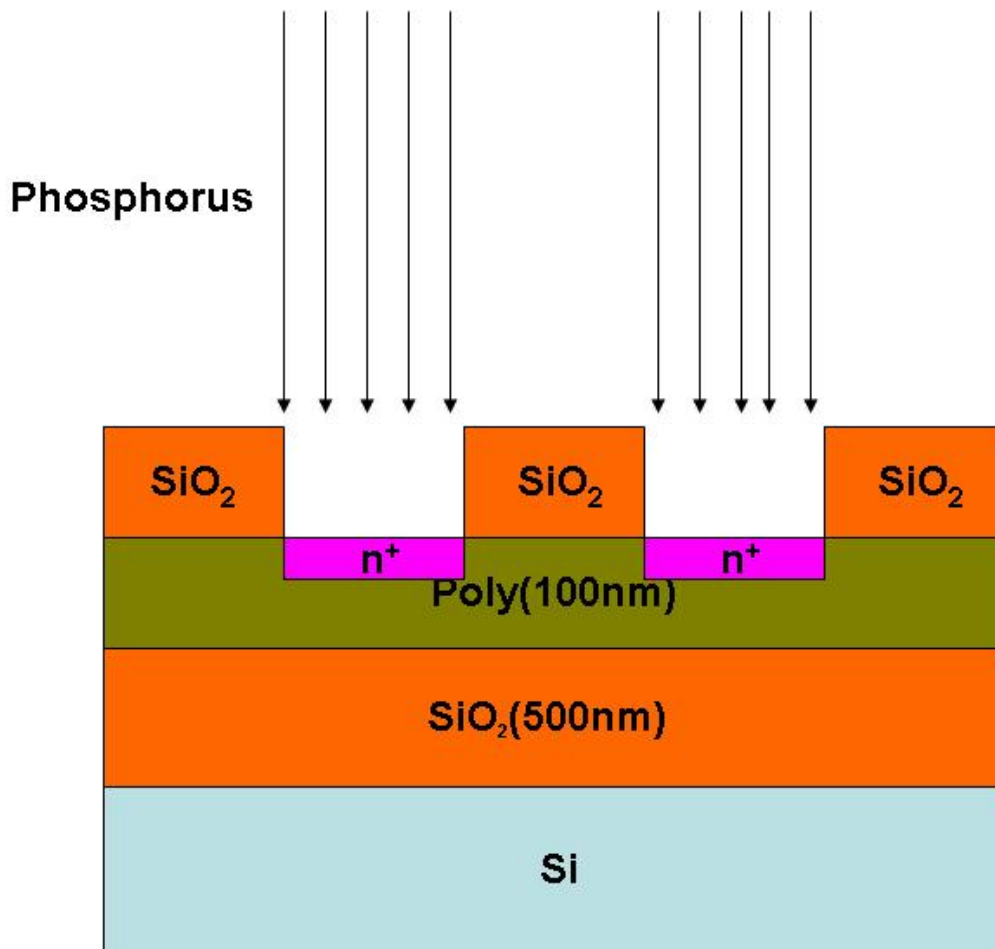
Fig 3.7 Step7

8. Activation in N_2 at 600^oC for 12hr.

9. Removing Silicon oxide on gate region (MASK-2)
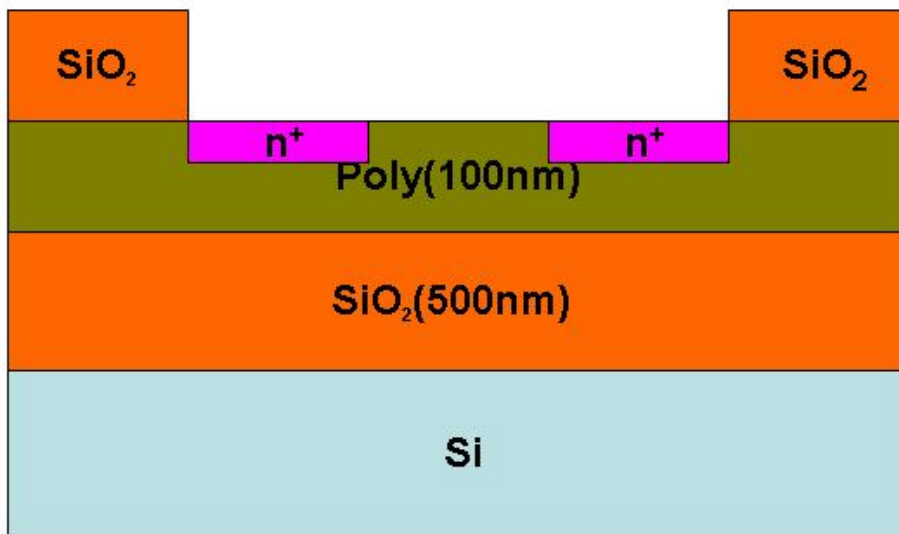
Fig 3.8 Step8

10. HfLaO deposition by PVD and 500°C PDA
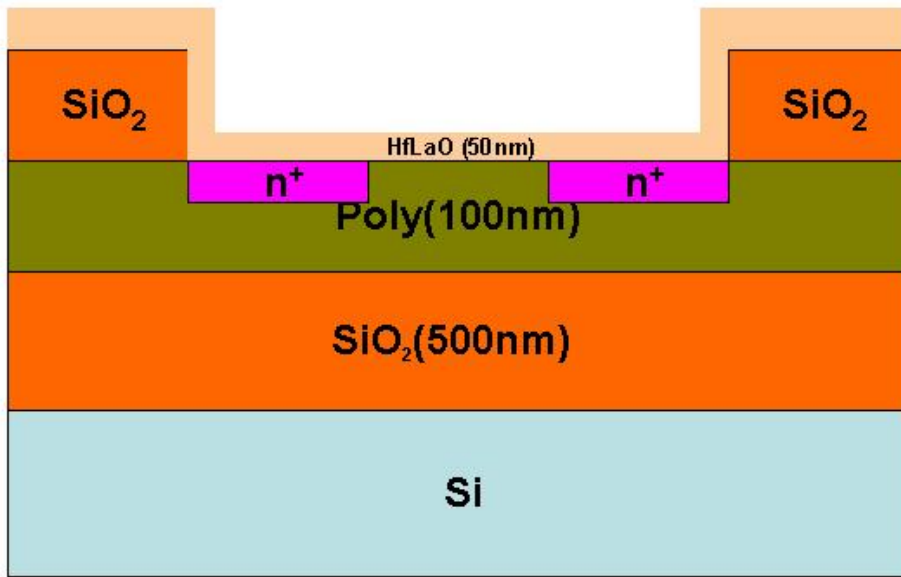
Fig 3.9 Step9

11. Contact hole, patterning, etching (MASK-3)
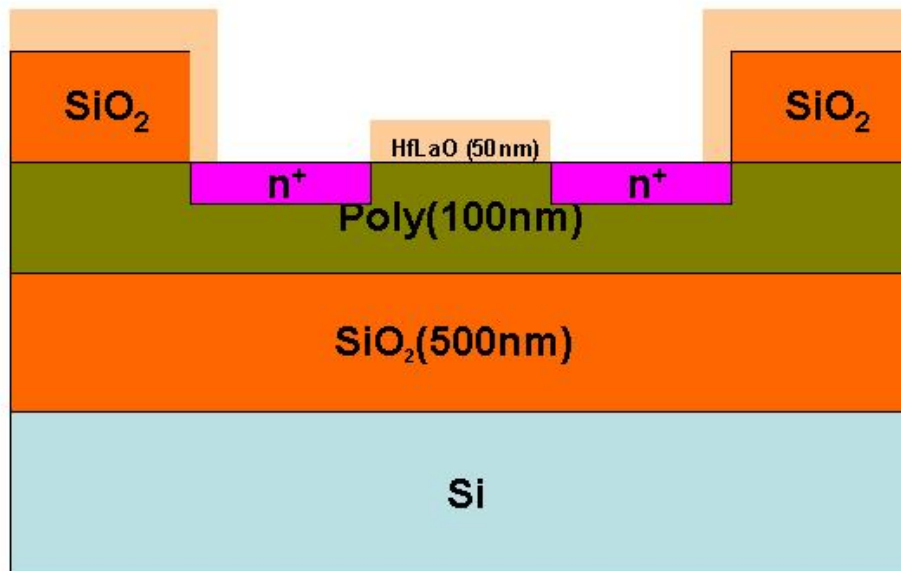
Fig 3.10 Step10

12. Photoresist deposition
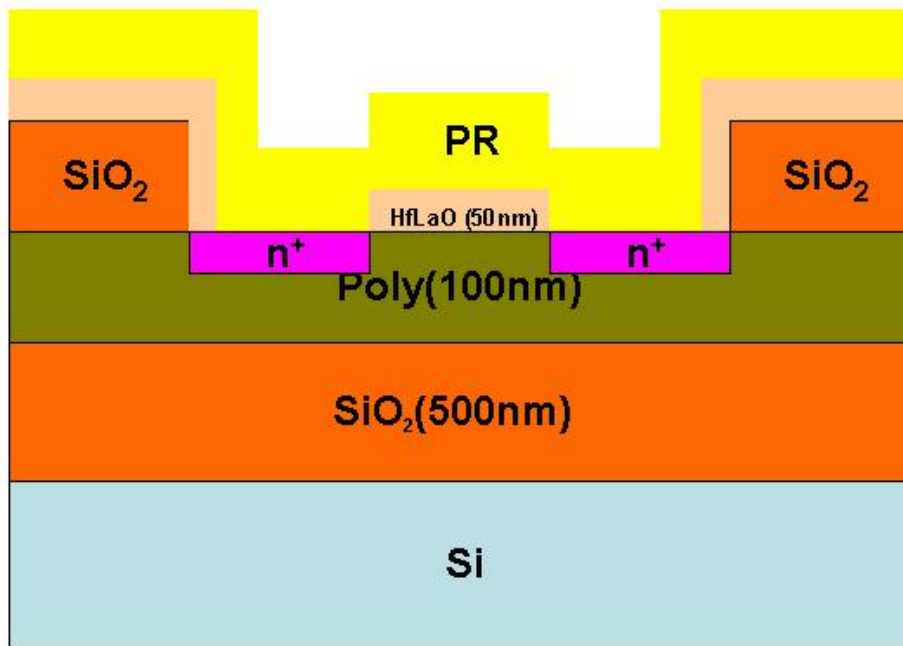
Fig 3.11 Step11

13. Metal region definition (lift-off, MASK-4)
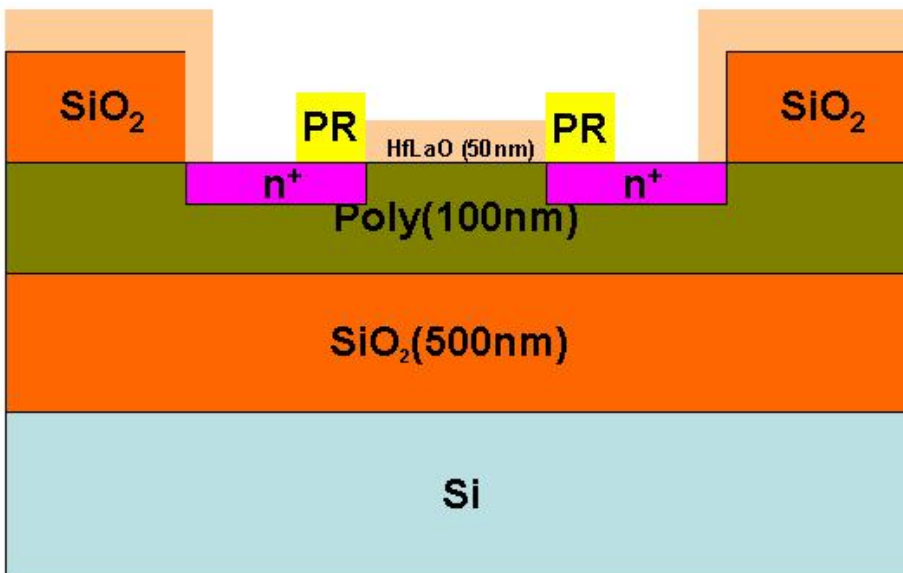
Fig 3.12 Step12

14. PVD-Al deposition (150nm)
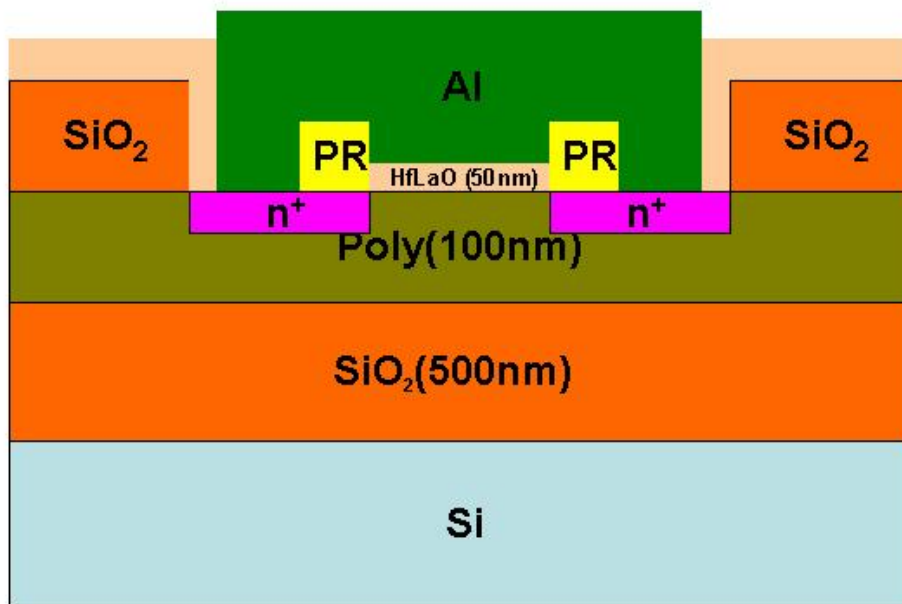
Fig 3.13 Step13

15. Removing PR
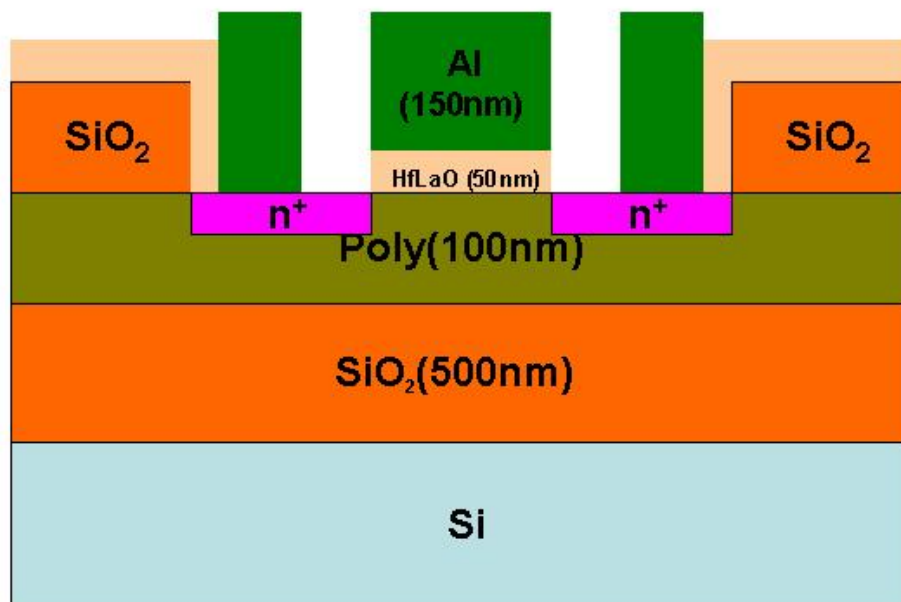
Fig 3.13 Step14

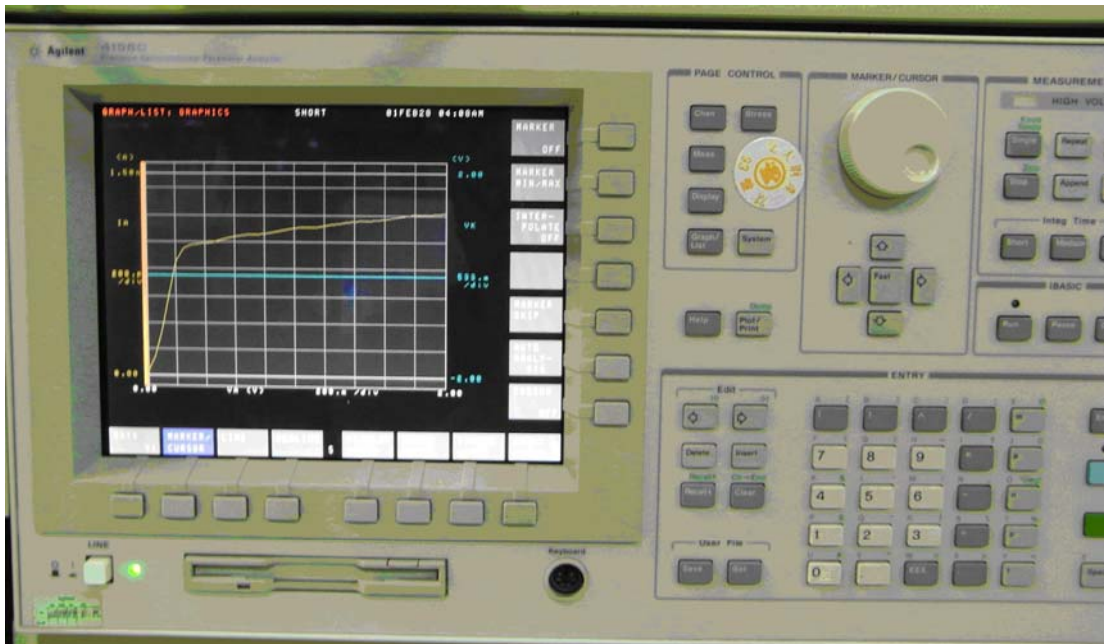**Fig 3.14 Probe station**

Fig 3.15 Agilent 4284

Fig 3.16 Agilent 4156

Chapter 4
Result & Discussion

## 4.1 **Experimental Data Result & Discussion**

The electrical characteristics of fabricated devices were measured by Agilent 4156

Precision Semiconductor Parameter Analyzer and Agilent 4284 LCR meter. The physical

thickness of these high-κ films were confirm by Ellipsometer. The first three Figures (Fig 4-1

~ Fig 4-3) show C-V characteristic of Al/HfLaO/Si capacitors with La ratio from 20% ~ 40%.

From the C-V curve, we get the EOT of HfLaO is around 8.5 ~ 9.1 nm, which is the thinnest

reported EOT in the application of TFTs so far. Combining the EOT with a physical thickness

of 50 nm, the dielectric constant of this PVD HfLaO is about 22, which is a high value to

overcome the more severe gate leakage current problem compared to MOSFETs. The

normalized C-V curve of Al/HfLaO/Si capacitors different La ratio from 20% ~ 40% were

shown in Fig. 4.4. It is obvious that the flatband voltage was more negative with the increase

of contained La. The output characteristics (I_d-V_d) of the Al/HfLaO TFTs with channel length

of 10 μm are shown from Fig. 4.5 to Fig. 4.7 . The large drive current of 800 ~ 1200 μA at 5V

is attractive for high-speed display ICs. The threshold voltage of our devices were extracted

using the method of tangent line on the I_d-V_g curve at the point of maximum transconductance

(Fig 4.8 ~ Fig4.10).   For each devices of La concentration 20%, 30%, 40% respectively, the

threshold voltage were 1.13V, 1V, 0.835V which is better than the threshold voltage of the

device with different dielectric materials which were reported before (Table 4.1). The

threshold voltage decreases because that La in the dielectric makes the more negative flatband

voltage . Base on the threshold voltage equation:

$$V_{TN} = \frac{\left(\left| Q'_{SD}(\max) \right| \right)}{C_{ox}} + V_{FB} + 2\phi_{fp}$$

More negative V_{FB} makes lower threshold voltage. And in Fig 4.11 ~ Fig 4.13, we can see

the sub-threshold slope of nearly 500 mV/decade, giving the good electron field-effect

mobility of 30.79 cm^2/Vs (for La/La+Hf = 40%) for all these devices. The good sub-threshold

swing and mobility indicate a low interface trap density. The I$_{on}$ / I$_{off}$ ratio of the Al/HfLaO

TFT is about 10^6, even without performing hydrogen passivation. This good performance is

related to the lower threshold voltage and the high gate-capacitance of from C-V

measurements, which gives a small equivalent-oxide thickness (EOT) and a high κ value ,

And the high drive current is higher than compared to other reported thin film transistor

(Table 1). It is because the Lanthanide in the high-κ layer makes the flat band voltage very

lower even using aluminum as the gate electrode which work function is 4.1eV. So the data

affirm our conception. Our design also provides an alternative way to create high drive

current, along with existing approaches such as excimer-laser crystallization (ELC),

metal-induced lateral crystallization and electric field enhanced crystallization. It shows that

good uniformity is also obtained due to the furnace crystallization, in contrast with the narrow

process window and poor uniformity in ELC TFTs. The field dependence of the gate current

density is showed in Fig 4.14 ~ Fig 4.16 shows a gate dielectric breakdown electric field can

up to 7 MV/cm. This is high enough to drive a liquid crystal display. This high breakdown

field is comparable with or better than that for PECVD TEOS oxide. This is important for

achieving good dielectric reliability. It may arise from the robust quality of HfLaO film and

the plasma-free process used, which does not damage the gate dielectric. Hence integrating

high-κ gate dielectrics HfLaO into TFT-NMOS should not degrade the TFT device reliability,

often dominated by the grain-boundary related hot-carrier degradation. The important device

parameters are summarized in Table 1. The better device performance of the Al/HfLaO TFTs

that compared with other structure is due to the lower threshold voltage which results from the

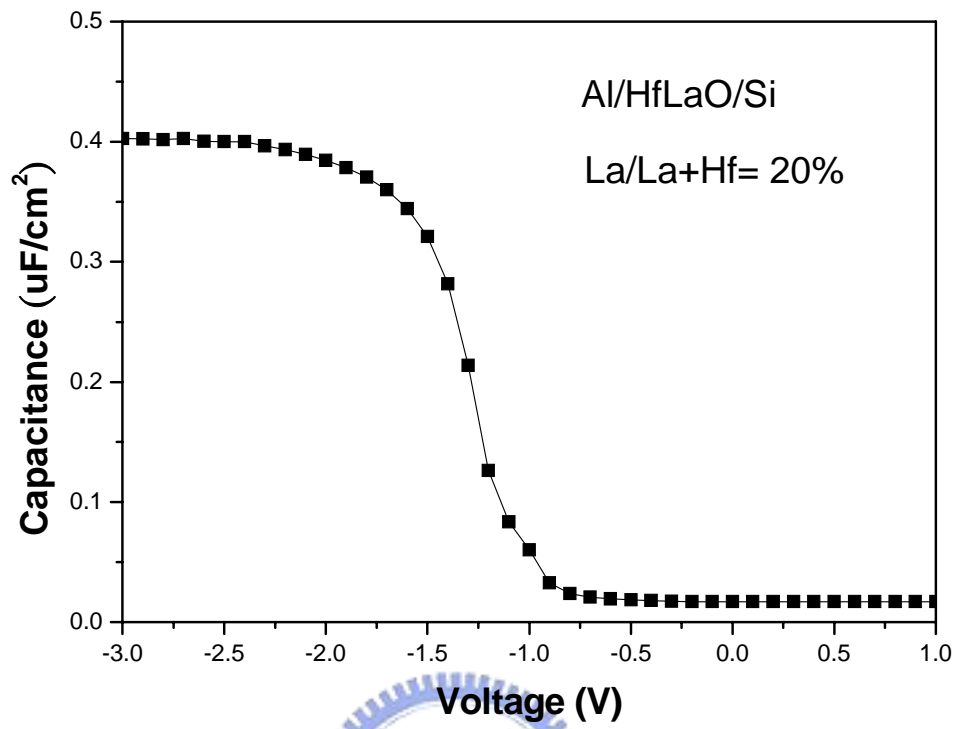higher capacitance density combining with the plasma-free process.
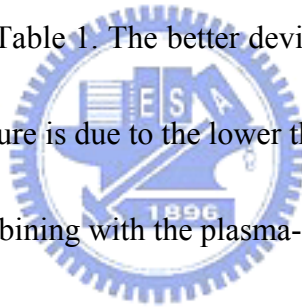
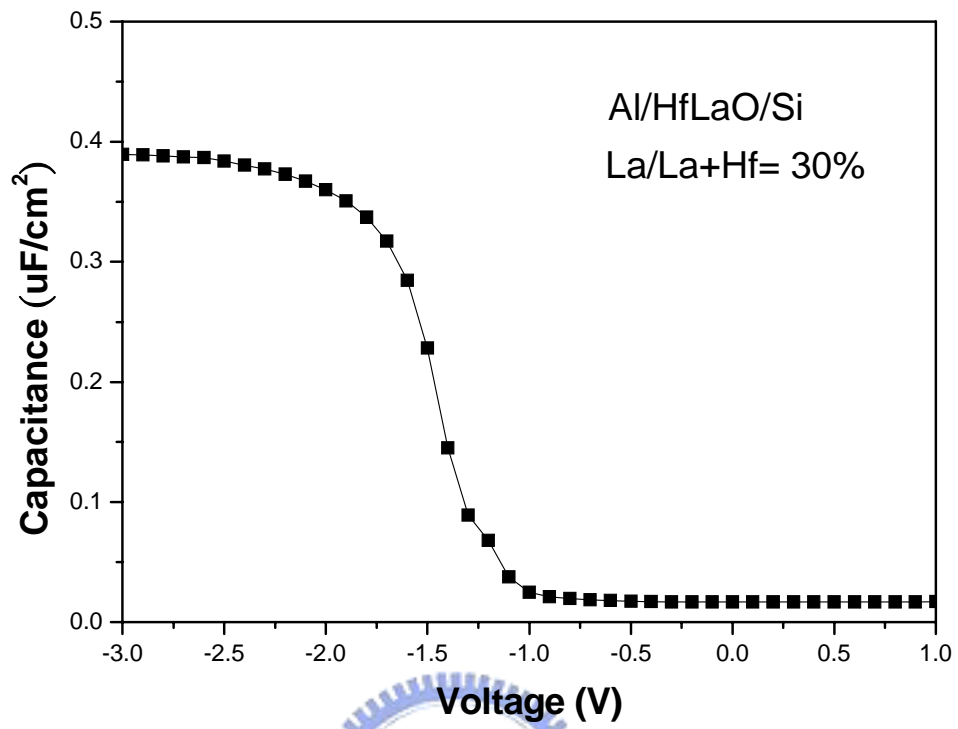**Fig 4.1 C-V of Al/HfLaO/Si capacitor with La ratio of 20%**

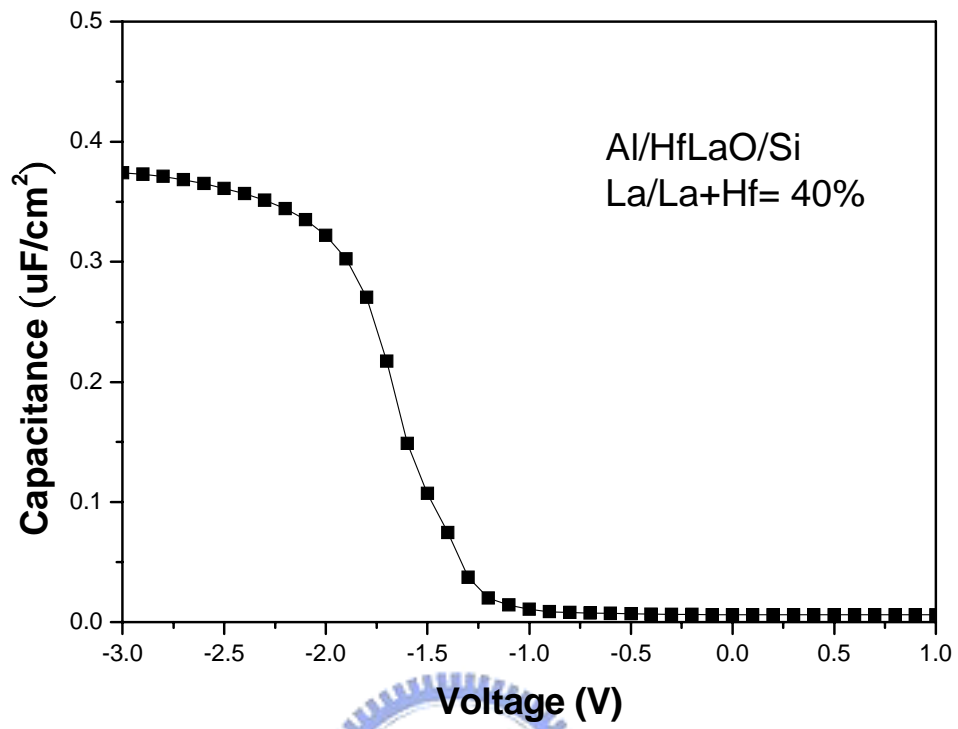Fig 4.2 C-V of Al/HfLaO/Si capacitor with La ratio of 30%

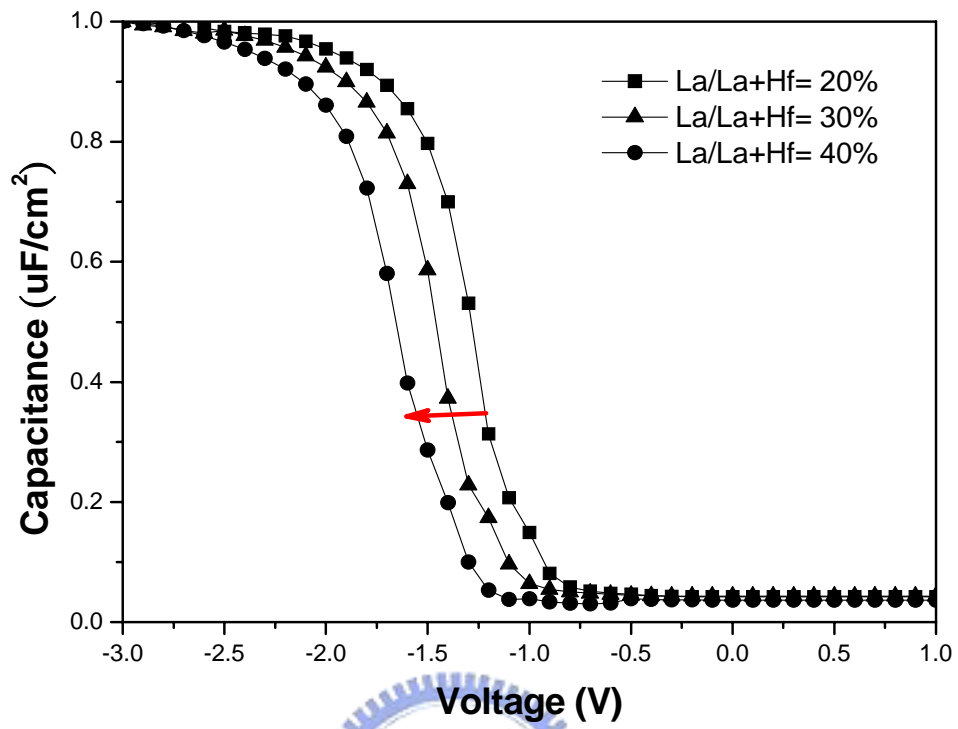Fig 4.3 C-V of Al/HfLaO/Si capacitor with La ratio of 40%

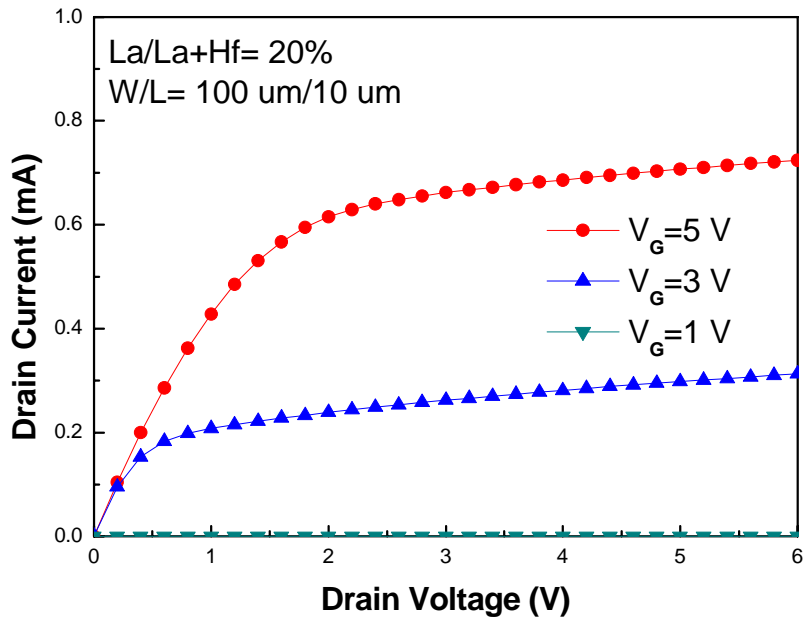**Fig 4.4 Normalized C-V of Al/HfLaO/Si capacitor with different La ratio from 20% ~**

40%

Fig 4.5 I$_d$-V$_d$ characterisitic of Al/HfLaO/Si TFT with La ratio of 20%
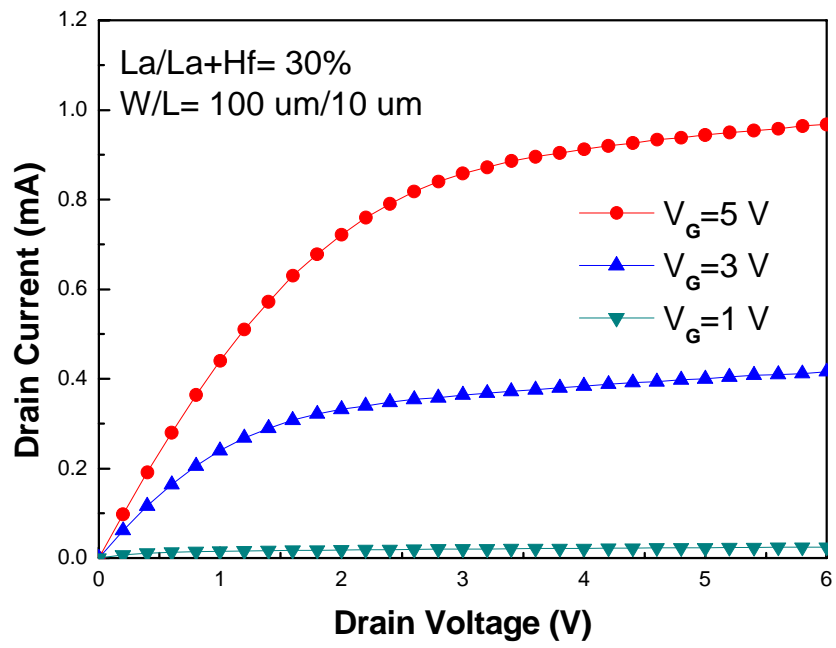
Fig 4.6 I$_d$-V$_d$ characterisitic of Al/HfLaO/Si TFT with La ratio of 30%
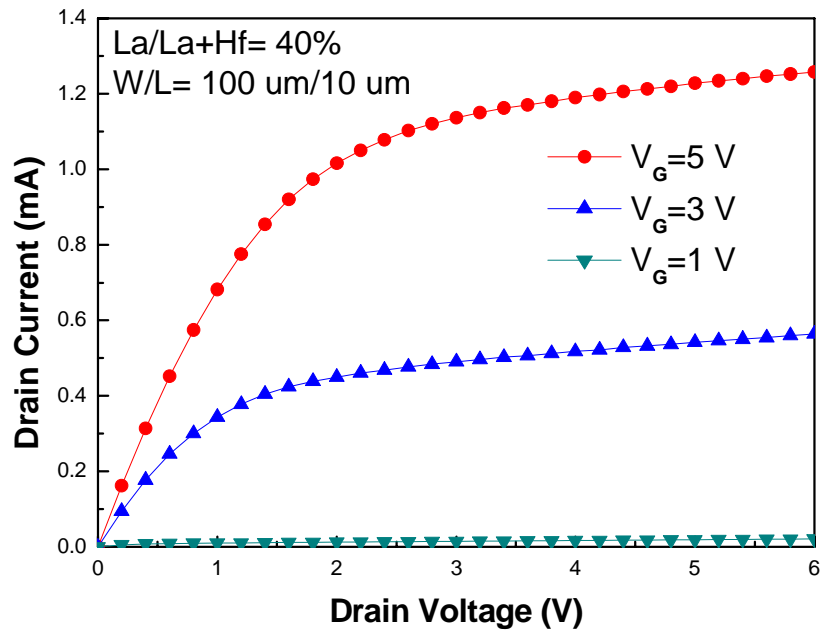
Fig 4.7 I_d-V_d characterisitic of Al/HfLaO/Si TFT with La ratio of 40%
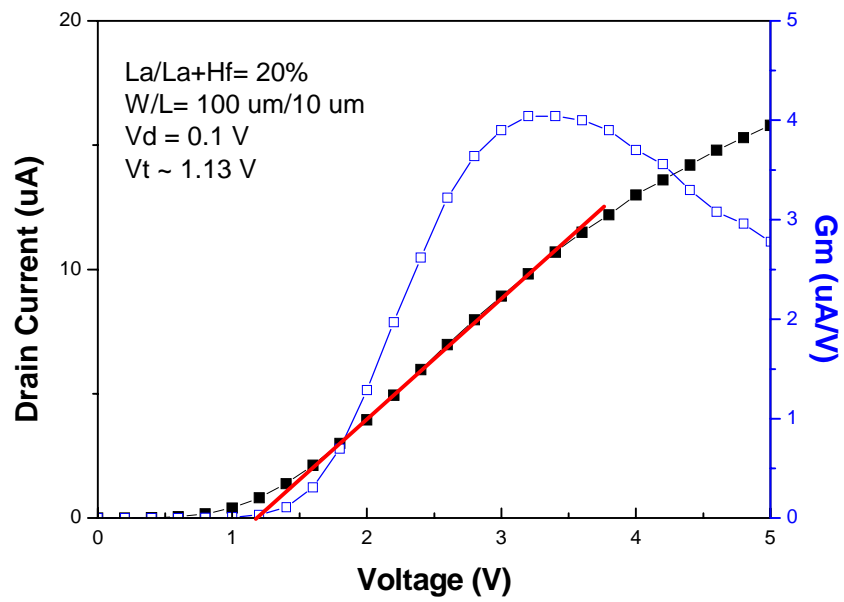
Fig 4.8 I_d-V_d and transconductacne characterisitic of Al/HfLaO/Si TFT with La ratio of
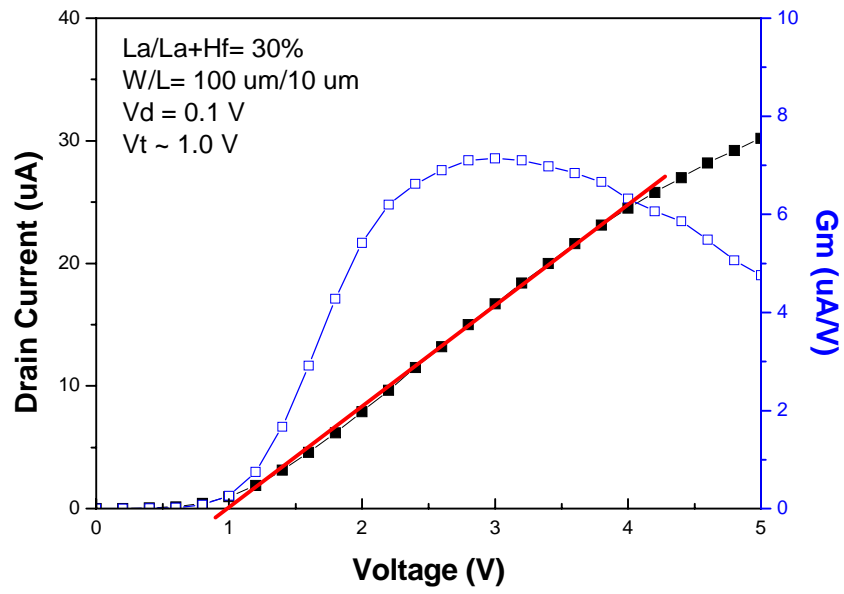
20%

Fig 4.9 I_d-V_d and transconductacne characterisitic of Al/HfLaO/Si TFT with La ratio of

30%

La/La+Hf= 40%
W/L= 100 um/10 um
Vd = 0.1 V
Vt ~ 0.835 V
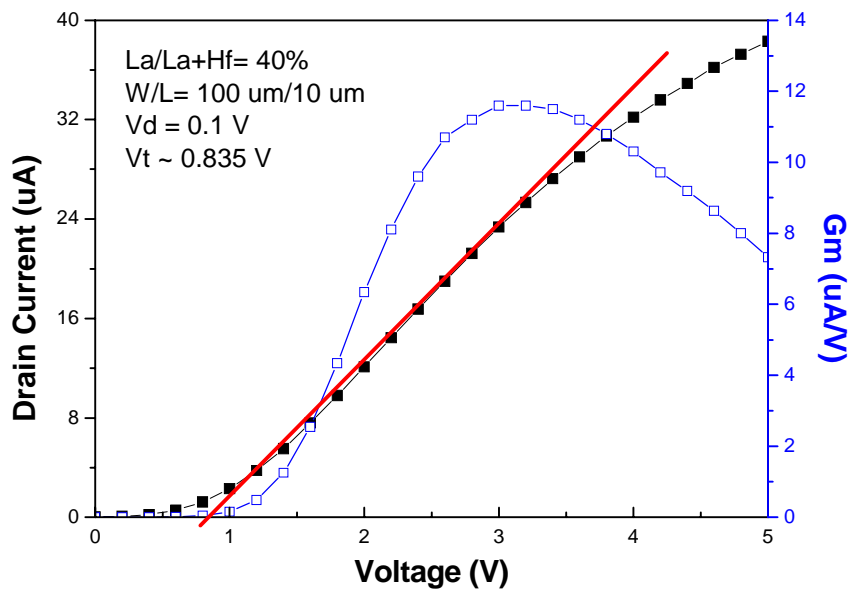
Fig 4.10 I_d-V_d and transconductacne characterisitic of Al/HfLaO/Si TFT with La ratio of

40%

La/La+Hf= 20%
W/L= 100 um/10 um
Vd = 0.1 V

Subthreshold Swing ~ 530 mV/dec
On/Off ratio ~ 1.2 x 10⁶

Fig 4.11 The low subshreshold slope of Al/HfLaO/Si TFT with La ratio of 20%

La/La+Hf= 30%
W/L= 100 um/10 um
Vd = 0.1 V

Subthreshold Swing ~ 518 mV/dec
On/Off ratio ~ 1.01 x 10^6

Fig 4.12 The low subshreshold slope of Al/HfLaO/Si TFT with La ratio of 30%

La/La+Hf= 40%
W/L= 100 um/10 um
Vd = 0.1 V

Subthreshold Swing = 508 mV/dec
On/Off ratio = 1.3 x 10^6

Fig 4.13 The low subshreshold slope of Al/HfLaO/Si TFT with La ratio of 40%

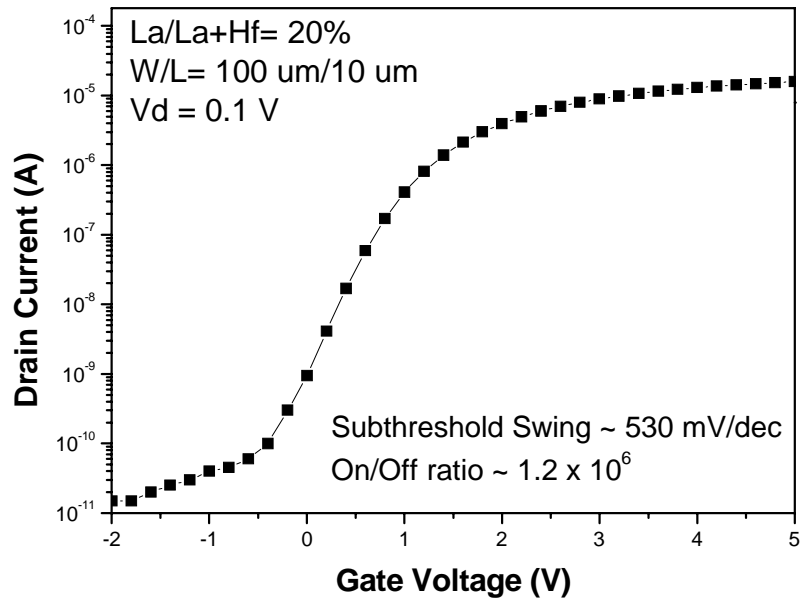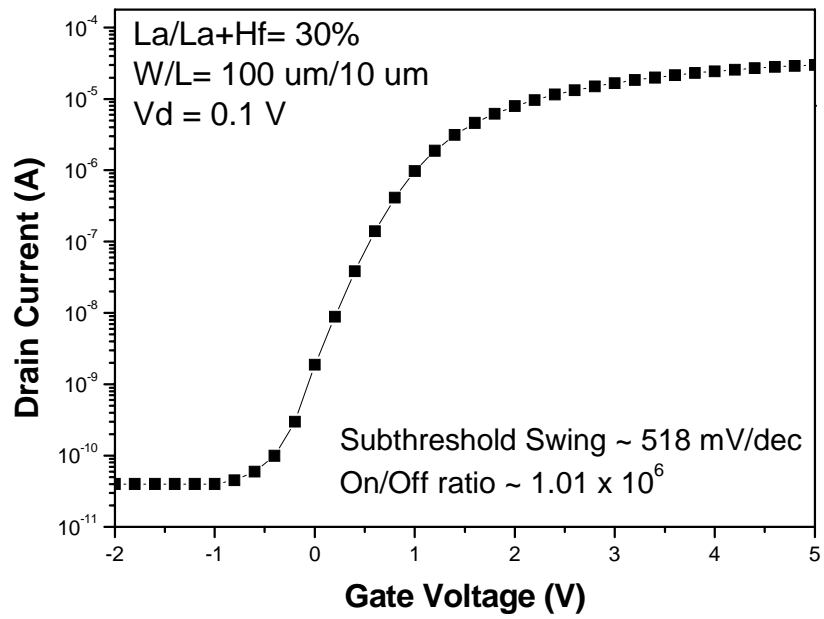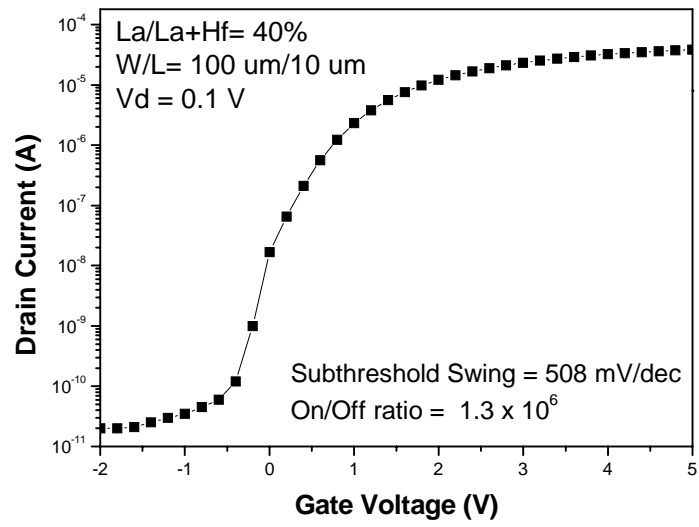**Fig 4.14 The breakdown voltage of Al/HfLaO/Si TFT with La ratio of 20%**

Al/HfLaO/Si
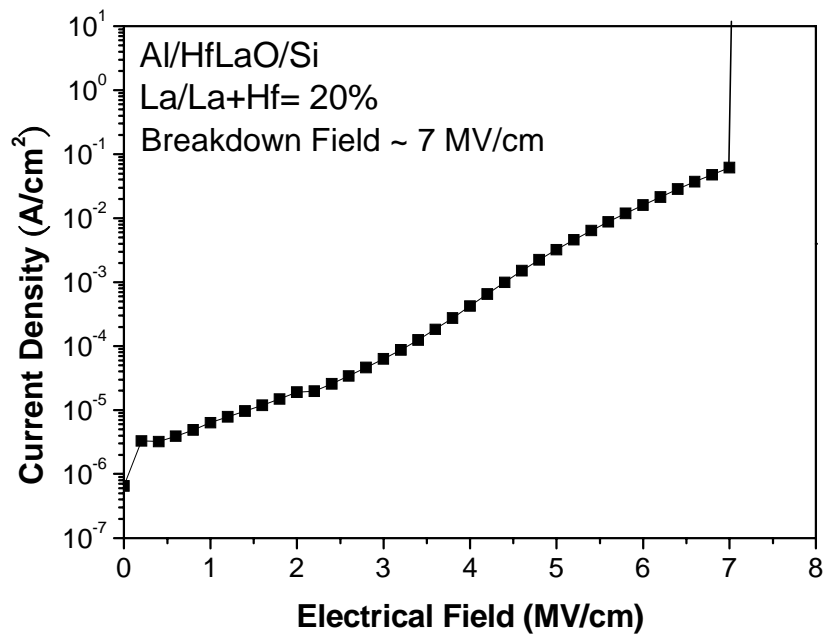La/La+Hf= 30%
Breakdown Field ~ 6.8 MV/cm
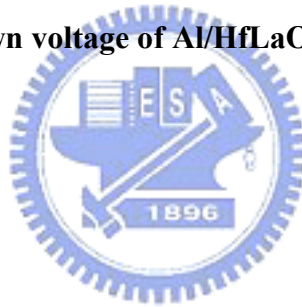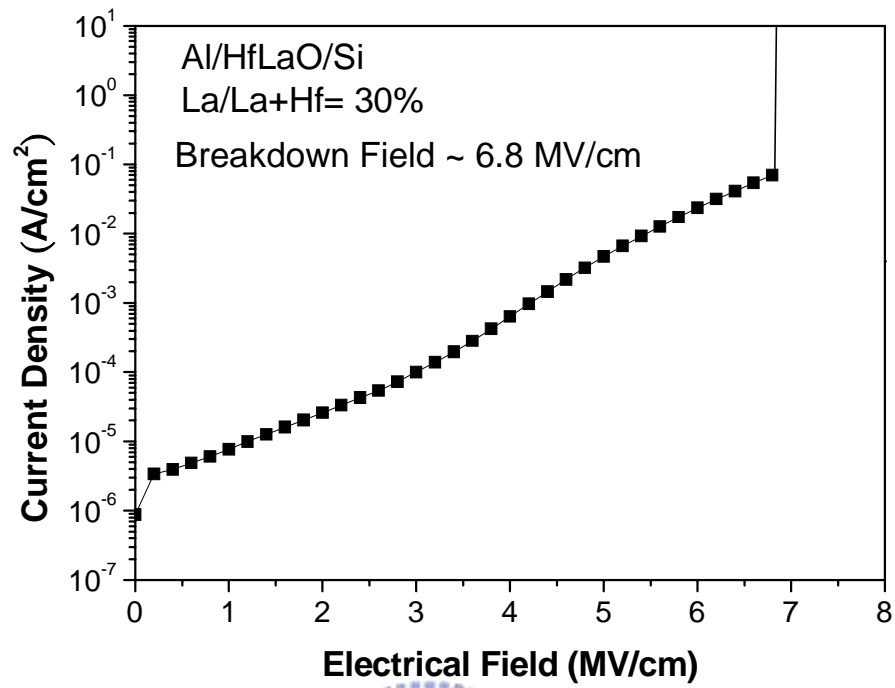
Fig 4.15 The breakdown voltage of Al/HfLaO/Si TFT with La ratio of 30%
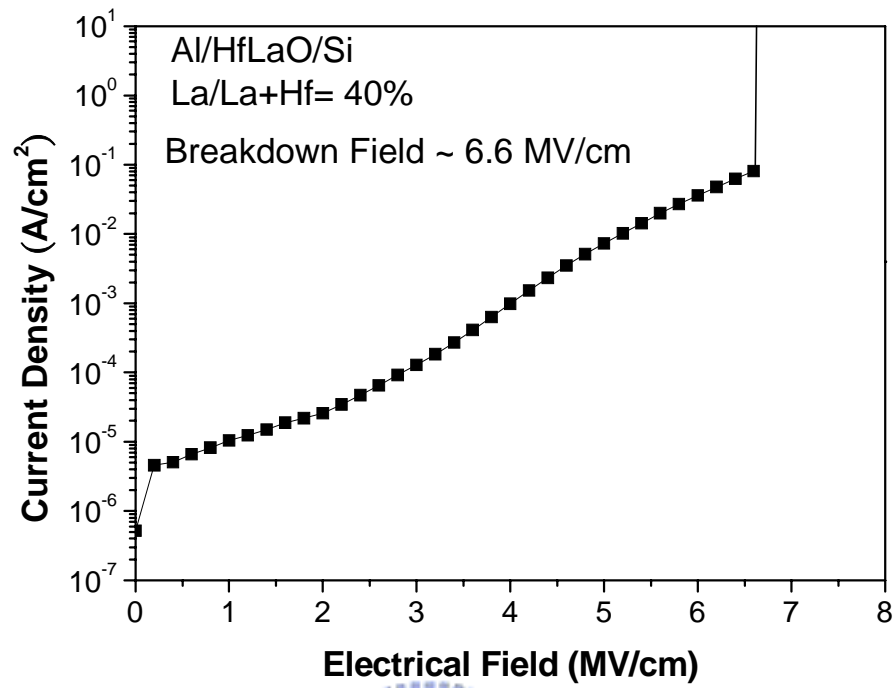
Fig 4.16 The breakdown voltage of Al/HfLaO/Si TFT with La ratio of 40%

Gate dielectric	This work HfLaO (La 40%)	LPCVD SiO$_2$ 80nm [28]	PECVD TEOS Oxide 60nm [29]	PECVD TEOS Oxide 40nm [30]	Al$_2$O$_3$ 50nm [30]
Gate electrode	Aluminum	Poly-Si	Poly-Si	Poly-Si	Poly-SiGe
V$_{th}$(V)	0.835	5.6	8.14	Not extracted	3
µFE (cm^2/V$_s$)	30.79	20	12.44	3	47
Sub-threshold Slope (V/decade)	0.508	1.4	1.97	2.67	0.44
I$_{on}$/I$_{off}$	1.3×10^6	3.5×10^5	2.97×10^5	Not extracted	3×10^5
Breakdown Field (MV/cm)	6.6	Not extracted	Not extracted	5.4	Not extracted

Table 1

Chapter 5
Conclusion

A new high-κ dielectric TFT with HfLaO as the gate insulator structure has been proposed and successfully fabricated. The process is simple and compatible to conventional LTPS process. Our experimental data show that the new new high-κ dielectric TFT has higher turn-on current, on/off current ratio and excellent current saturation characteristics at high bias, compared to the conventional TFT. That is due to the high-κ value and robust quality of HfLaO film itself and the plasma-free process used, which does not damage the gate dielectric. The new structure is therefore ideally suitable for implementing high-density and high-performance driver circuits on the glass panel for AM-LCD applications. This is because that our TFT device has lower threshold voltage, low subthreshlod slope, high field effect mobility lower leakage current, good breakdown voltage, higher turn-on current and on/off current ratio.

Chapter 6
Reference

[1]   M. Koyama, K. Suguro, M. Yoshiki, Y. Kamimuta, M. Koike, M. Ohse, C. Hongo and A. Nishiyama, "Thermally stable ultra-thin nitrogen incorporated ZrO_2 gate dielectric prepared by low temperature oxidation of ZrN" in *IEDM Tech. Dig.,* 2001, pp. 20.3.1-20.3.4.

[2]   E. P. Gusev, D. A. Buchanan, E. Cartier, A. Kumar, D. DiMaria, S. Guha, A. Callegari, S. Zafar, P. C. Jamison, D. A. Neumayer, M. Copel, M.A. Gribelyuk, H. Okorn-Schmidt, C. D Emic, P. Kozlowski, K. Chan, N. Bojarczuk, L.-A. Ragnarsson and Rons, "Ultrathin high-κ gate stacks for advanced CMOS devices" in *IEDM Tech. Dig.*, 2001, pp. 20.1.1-20.1.4.

[3]   W.Zhu, T. P. Ma, T. Tamagawa, Y. Di, J. Kim, R. Carruthers, M. Gibson and T. Furukawa, "HfO_2 and HfAlO for CMOS: thermal stability and current transport" in *IEDM Tech. Dig.*, 2001, pp. 20.4.1-20.4.4.

[4]   L. Kang, K. Onishi, ?Y. Jeon, Byoung Hun Lee, C. Kang, Wen-Jie Qi, R. Nieh, S. Gopalan, R Choi and J. C. Lee, "MOSFET devices with polysilicon on single-layer HfO_2 high-κ dielectrics" in *IEDM Tech. Dig.*, 2000, pp.35-38

[5]   Rino Choi, Chang Seok Kang, Byoung Hun Lee, K. Onishi, R. Hieh, S. Gopalan, E. Dharmarjan and J. C. Lee, "High-quality ultra-thin HfO_2 gate dielectric

MOSFETs with TaN electrode and nitridation surface preparation" in *IEDM Tech. Dig.*, 2001, pp. 15-16.

[6] Z. J. Luo, T. P. Ma, E. Cartier, M. Copel, T. Tamagawa and B. Halpern, "Ultra-thin ZrO₂ (or silicate) with high thermal stability for CMOS gate applications" in *Symp on VLSI Technology*, 2001, pp. 135-136.

[7] International Technology Roadmap for Semiconductor, 2006.

[8] J. K. Schaeffer, C. Capasso, L. R. C. Fonseca, S. Samavedam, D. C. Gilmer, Y. Liang, S. Kalpat, B. Adetutu, H.-H. Tseng, Y. Shiho, A. Demkov, R. Hegde, W. J. Taylor, R. Gregory, J. Jiang, E. Luckowski, M. V. Raymond, K. Moore, D. Triyoso, D. Roan, B. E. White Jr, and P. J. Tobin, "Challenges for the integration of metal gate electrodes," in *IEDM Tech. Dig.*, 2004, pp. 287-290

[9] W. P. Maszara, Z. Krivokapic, P. King, J. S. Goollgweon, and M. R. Lin, "Transistors with dual work function metal gate by single full silicidation (FUSI) of polysilicon gates," in *IEDM Tech. Dig*, 2002, pp.367-370.

[10] H.-H. Tseng, C. C. Capasso, J. K. Schaeffer, E. A. Hebert, P. J. Tobin, D. C. Gilmer, D. Triyoso, M. E. Ramón, S. Kalpat, E. Luckowski, W. J. Taylor, Y. Jeon, O. Adetutu, R. I. Hegde, R. Noble, M. Jahanbani, C. El Chemali, and B. E. White, "Improved short channel device characteristics with stress relieved pre-oxide (SRPO) and a novel tantalum carbon alloy metal gate/HfO2 stack," in

IEDM Tech. Dig., pp. 821-824, 2004.

[11] H. -J. Cho, C. S. Kang, K. Onishi, S. Gopalan, R. Nieh, R. Choi, E. Dharmarajan and J.C. Lee, " Novel nitrogen profile engineering for improved TaN/HfO2 Si MOSFET performance," in *IEDM Tech. Dig.*, pp. 30.2.1-30.2.4, 2001.

[12] Y. T. Hou, M. F. Li, T. Low, and D. L. Kwong, " Impact of metal gate work function on gate leakage of MOSFETs," in *DRC Symp.*, pp. 154-155, 2003.

[13] Dae-Gyu Park, Kwan-Yong Lim, Heung-Jae Cho, Tae-Ho Cha, Joong-Jung Kim, Jung-Kyu Ko, Ins-Seok Yeo and Jin Won Park, " Novel damage-free direct metal gate process using atomic layer deposition," in *Symp. on VLSI Technology*, pp. 65-66, 2001.

[14] C. Cabral Jr. , J. Kedzierski, B. Linder, S. Zafar, V. Narayanan, S. Fang, A. Steegen, P. Kozlowski, R. Carruthers, and R. Jammy," Dual workfunction fully silicided metal gates," in *Symp. on VLSI Technology*, pp. 184-185, 2004.

[15] S. B. Samavedam, L. B. La, J. Smith, S. Dakshina-Murthy, E. Luckowski, J. Schaeffer, M. Zavala, R. Martin, V. Dhandapani, D. Triyoso, H. H. Tseng, P. J. Tobin, D. C. Gilmer, C. Hobbs, W. J. Taylor, J. M. Grant, R. I. Hegde, J. Mogab, C. Thomas, P. Abramowitz, M. Moosa, J. Conner, J. Jiang, V. Arunachalarn, M. Sadd, B.-Y. Nguyen, and B. White," Dual-metal gate CMOS with HfO2 gate dielectric," in *IEDM Tech. Dig.*, pp. 433-436, 2002.

[16] D. S. Yu, A. Chin, C. C. Laio, C. F. Lee, C. F. Cheng, W. J. Chen, C. Zhu, M.-F. Li, S. P. McAlister, and D. L. Kwong, "3D GOI CMOSFETs with novel IrO2 (Hf) dual gates and high-   dielectric on 1P6M-0.18   m-CMOS," in *IEDM Tech.*

Dig., pp. 181-184, 2004.

[17] D. S. Yu , A. Chin, C. C. Liao, C. F. Lee, C. F. Cheng, M. F. Li, Won Jong Yoo, and S. P. McAlister, "3D Metal-Gate/High- /GOI CMOSFETs on 1-Poly-6-Metal 0.18-um Si Devices," *IEEE Electron Device Lett*. 26, pp. 118-120, Feb. 2005.

[18] X. P. Wang, C. Shen, Ming-Fu Li, H.Y. Yu, Yiyang Sun, Y. P. Feng, Andy Lim, Hwang Wan Sik, Albert Chin, Y. C. Yeo, Patrick Lo, and D.L. Kwong," Dual Metal Gates with Band-Edge Work Functions on Novel HfLaO High- Gate Dielectric," in *Symp. on VLSI Technology*, pp. 12-13, 2006.

[19] J. H. Lee, H. Zhong, Y.-S. Suh, G. Heuss, J. Gurganus, B. Chen, and V. Misra," Tunable work function dual metal gate technology for bulk and nonbulk CMOS," in *IEDM Tech. Dig*., pp. 359-362, 2002.

[20] H. Y. Yu, M. F. Li, and D.L. Kwong," Thermally Robust HfN Metal as a Promising Gate Electrode for Advanced MOS Device Application," *IEEE Transactions on Electron Devices*, vol. 51, Apr., 2004.

[21] A. Veloso, K. G. Anil, L. Witters, S. Brus, S. Kubicek, J.-F. de Marneffe, B. Sijmus, K. Devriendt, A. Lauwers, T. Kauerauf, M. Jurczak, and S. Biesemans, "Work function engineering by FUSI and its impact on the performance and reliability of oxynitride and Hf-silicate based MOSFETs," in *IEDM Tech. Dig*., pp. 855-858, 2004.

[22] S. J. Rhee, C. S. Kang, C. H. Choi, C. Y. Kang, S. Krishnan, M. Zhang, M. S. Akbar, and J. C. Lee, "Improved electrical and material characteristics of hafnium titanate multi-metal oxide n-MOSFETs with ultra-thin EOT (~8Å) gate dielectric application," in *IEDM Tech. Dig*., pp.837-840, 2004.

[23] K. C. Chiang, A. Chin, C. H. Lai, W. J. Chen, C. F. Cheng, B. F. Hung,and C. C.

Liao, "Very high _ and high density TiTaO MIMcapacitorsfor analog and RF applications," in *Symp. VLSI Tech. Dig*., 2005, pp.62–63.

[24] D. S. Yu, A. Chin, C. H. Wu, M.-F. Li, C. Zhu, S. J. Wang, W. J. Yoo, B. F. Hung, and S. P. McAlister, "Lanthanide and Ir-based dual metalgate/ HfAlON CMOS with large work-function difference," in *IEDM Tech. Dig*., 2005, pp. 649–652.

[25] C. H. Huang, D. S. Yu, A. Chin, W. J. Chen, C. X. Zhu, M.-F. Li, B. J. Cho, and D. L. Kwong, "Fully silicided NiSi and germanided NiGe dual gates on SiO2/Si and Al2O3/Ge-on-insulator MOSFETs," in IEDM Tech. Dig., 2003, pp. 319–322.

[26] B. Tavel, T. Skotnicki, G. Pares, N. Carrière, M. Rivoire, F. Leverd, C. Julien, J. Torres, and R. Pantel, "Totally silicided (CoSi2) polysilicon: A novel approach to very low-resistive gate (∼2Ω/_) without metal CMP nor etching," in IEDM Tech. Dig., 2001, pp. 815–828.

[27] T. Nabatame, M. Kadoshima, K. Iwamoto, N. Mise, S. Migita, M. Ohno, H. Ota, N. Yasuda, A. Ogawa, K. Tominaga, H. Satake, and A. Toriumi, "Partial silicides technology for tunable work function electrodes on high-κ gate dielectrics-fermi level pinning controlled PtSix for HfOx(N) pMOSFET," in IEDM Tech. Dig., 2004, pp. 83–86.

[28] Y. W. Choi, J. N. Lee, T. W. Jang, and B. T. Ahn, "Thin-film transistors fabricated with poly-Si films crystallized at low temperature by microwave

annealing," *IEEE Electron Device Lett.*, vol. 20, pp. 2-4, Jan. 1999.

[29] C. W. Lin, M.Z. Yang, C. C. Yeh, L. J. Cheng, T. Y. Huang, H. C. Cheng, H. C. Lin, T. S. Chao, C. Y. Chang, "Effects of plasma treatments, substrate types, and crystallization methods on performance and reliability of low temperature polysilicon TFTs"in *IEDM Tech. Dig.*, 1999, p. 305-308.

[30] K. M. Chang, W. C. Yang, and C. P. Tsai, "Electrical characteristics of low temperature polysilicon TFT with a novel TEOS/oxynitride stack gate dielectric," *IEEE Electron Device Lett.*, vol. 24, pp. 512-514, Aug. 2003.

[31] Z. Jin, H. S. Kwok, and M. Wong, "High-performance polycrystalline SiGe thin-film transistors using Al2O3 gate insulators," *IEEE Electron Device Lett.*, vol. 19, pp. 502-504, Dec. 1998.

Vita

姓名：黃群懿

性別：男

出生年月日：民國69年1月28日

籍貫：台北縣

住址：新竹縣新埔鎮南平里南平路349巷40號

學歷：私立亞東技術學院電子工程系

　　　（91年9月~95年1月）

　　　國立交通大學電機學院微電子奈米產業研發碩士班

　　　（95年2月~97年1月）

論文題目：

低臨限電壓與高驅動電流之薄膜電晶體在金屬鋁與介電層氧化鑭鉿上之研究

Low Threshold Voltage and High Drive Current Poly-Silicon Thin Film Transistors Using Aluminum Metal Gate and HfLaO Dielectric